Hobbing and Grinding Process Modelling of Helical Wheel in The Speed Reducer of an Electric Vehicle

Master's Thesis in Mechanical Engineering

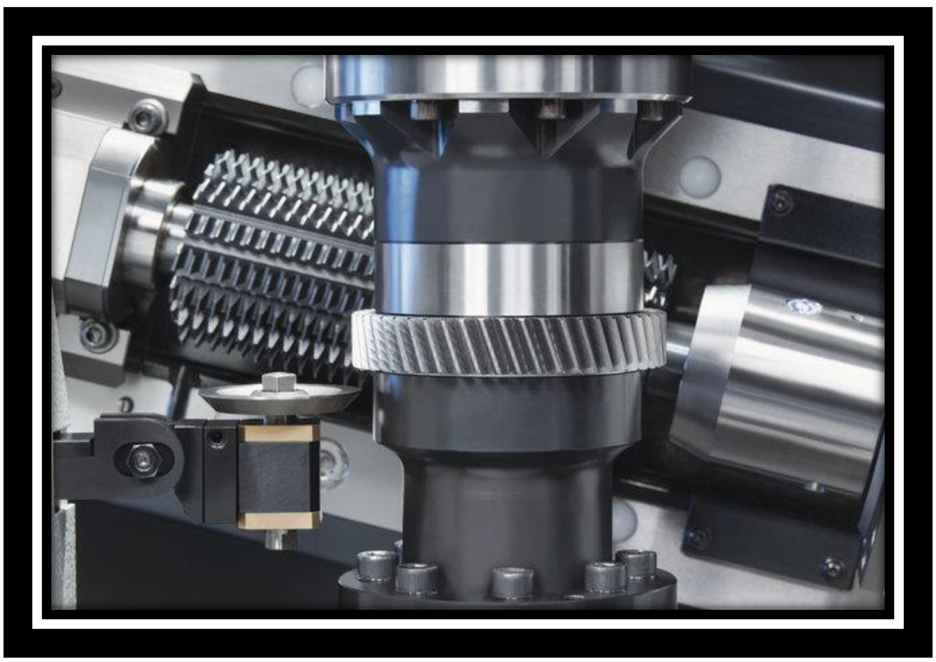

Supervisors: Jérôme BRUYERE François GIRARDIN
Tutor: Francesca Maria CURÀ
Grad student: Nagelaa ES SAFIANI

MASTER'S THESIS IN MECHANICAL ENGINEERING

Hobbing and Grinding Process Modelling of Helical Wheel in The Speed Reducer of an Electric Vehicle

Nagelaa ES SAFIANI

Department of Mechanical Engineering
Division of Industrialization and Processes
National Institute of Applied Sciences of Lyon
Lyon, France 2019

Department of Mechanical Engineering
Division of Production
Polytechnic University of Turin
Turin, Italy 2019

Abstract

When developing a mechanical transmission one important characteristic of the transmission is how much tonal noise and vibrations are generated. The vibrations causing are called gear whine noise and they are generated in the gear contacts of the transmission and propagate through the shafts and bearings to the housing, where they become airborne. In electrical vehicle applications the absence of a loud combustion engine makes the gear whine noise more distinct and easily perceived by the human ear. The main cause of the noise has been assumed to be excitations due to variations of tooth profile errors in the wheel of speed reducer. For this reason, a code to simulate the hobbing and grinding process, that generates the helical wheel, has been developed by the MATLAB software. To write the code, a kinematic study about hobbing and grinding process has been performed, then it has been possible to obtain the theoretical points of contact on wheel surface and hob surface. After obtaining the programming code, it will be possible to compare the theoretical and real surfaces and analyse the possible causes.

Résumé

Pendant le développement d'une transmission mécanique il est important de maitriser le bruit et les vibrations générées. Le spectre de ces signaux peut faire apparaitre certaines fréquences indépendantes de la fréquence d'engrènement. Elles sont appelées raies fantômes et sont générées par le contact entre les roues d'une transmission. Elles sont transmises à travers les arbres et les roulements vers le carter. Dans un véhicule électrique, l'absence de moteur thermique fait que le bruit est plus perceptible pour les personnes. Les erreurs de fabrication de profil des roues sont considérées comme la causes principales de ce bruit. Pour cette raison et, par le moyen d'un code MATLAB, le processus de taillage et le processus de rectification ont été simulés. Pour le développement du code, on a étudié la cinématique de taillage et de rectification pour obtenir les points de contact théorique sur la surface de la roue et sur la surface de la fraise. Par la suite, il sera possible de comparer les surfaces théoriques et les surfaces réelles de la roue pour essayer de comprendre les causes du bruit.

Acknowledgements

I would like to thank my supervisors Francois Girardin and Jerome Bruyere for their great help and guidance throughout this thesis, for the continuous support of my Master study and related research, for their patience, motivation, and knowledge. Many thanks to the staff of *Groupe PSA* for their time and sharing of knowledge. I would also like to give thanks to my referent Francesca Maria Curà for taking care of me during my academic mobility.

I must express my very profound gratitude to my parents and my sister for providing me with unfailing support and continuous encouragement throughout my years of study and through the process of researching and writing this thesis. A special gratitude to Imad for his patience and help, this accomplishment would not have been possible without him.

Finally, I would like to thank God to have given me a life full of love.

Nagelaa Es Safiani

Contents

Nomenclature

α_n real pression angle
α_t apparent pression angle
a tip level
A amplitude angular deviation
ß helix angle
$ß_a$ feed motion angle
$ß_b$ base helix angle
b tooth width
C interaxial distance
C_a addendum modification coefficient
C_f dedendum modification coefficient
C_f profile control
C_{fu} effective dedendum modification coefficient
D pitch diameter
d_a tip diameter
d_b base diameter
d_f root diameter
ε defect
e eccentricity
φ cylindrical coordinate
F_a tip form
$F_{f\alpha}$ profile form deviation
$F_{fß}$ helix form deviation
f_h hob feed motion per turn
$f_{H\alpha}$ profile slope deviation
$f_{Hß}$ helix slope deviation
F_α total profile deviation
$F_ß$ total helix deviation
g_α length of path of contact
i tooth number
k flute number
$\lambda_ß$ wavelength undulation
L_α profile evaluation length

L_β helix evaluation length
m_n real module
m_t apparent module
na feed motion direction
Nbg number of hob flutes
N_f start of active profile
Ω_h hob angular speed
Ω_p pinion angular speed
p circle pitch
ρ coefficient of tooth side
r pitch radius
r_a tip radius
r_b base radius
r_f root radius
R_h hob mobile referent system
R_{h0} hob fix referent system
R_p pinion mobile referent system
R_{p0} pinon fixe referent system
S angle between rotation axes of pinion and hob
s linear extension of the teeth on the action plane
s_n real thickness
s_t apparent thickness
s_{tb} base apparent thickness
τ_ε defect torsor
Θ_h hob angular position
Θ_p pinion angular position
V_h feed motion speed
x_0 eccentricity error
x_1 pinion profile shift coefficient
x_2 hob profile shift coefficient
Z_{eq} speed ratio
z_h number of hob fillets
z_p number of pinon teeth

1
Introduction

The project is carried out for the *Groupe PSA* company known Peugeot S.A. Is a French multinational manufacturer of automobiles and motorcycles. The object of study is the helical tooth in the gearbox of an electric vehicle. The transmission of a gear normally presents noises that depend on the meshing frequency between the gear teeth and its harmonics, then they are remark frequencies. This noise phenomenon can be controlled since the theoretical geometric definition of the helical tooth. Noise from electric vehicles is an important environmental issue and several sources contribute to the tonal noise level. The tonal noise from the gearbox can be very disturbing for the driver, even if the noise level from the gearbox is lower than the total noise level. The human ear has a remarkable way of detecting pure tones of which the noise from loaded gears. The gearbox can be an important contributor to the total noise level[1]. Some tonal noises can occur, which are not directly linked to the geometric definition of the helical wheel, one hypothesis is that the problem is linked to the surface texture. With surface texture we mean the post-treatment processes to reinforce the component and all manufacturing process to have the tooth profile. In order to better control tonal sources which could eventually lead to undesirably high levels of gear whine, one need is to better understand and if possible, to model all those manufacturing processes that affect the mechanical performance of the component. From the cutting process, to the grinding process to thermal-treatment processes.

1.1 Objetcives

In order to proceed with the analysis of the mechanical problem therefore necessary to study the kinematics of the machines used to manufacturing the helical gear, the kinematics of the cutting machine, the kinematics of the grinding machine and the others possible manufacturing processes of the component. By studying the kinematics of manufacturing machines, it is possible to achieving the nominal geometry of the component and then to possible geometrical and surface finishing problems. After analyzing the nominal geometry of the helical tooth, different errors will be introduced to observe the behavior of the component in the transmission. We will analyze errors concerning the surface finishing and errors related to assembly. Will be done a comparison between the different surfaces finishing related to various errors introduced and the respective results.

2

Review of Literature

This chapter explains what a mechanical transmission is and how it is used in the automotive sector. In the automotive sector there are different types of mechanical transmissions, therefore the most common in the industrial field will be explained.

2.1 Mechanic Transmission

A transmission is a machine in a power transmission system, which provides controlled application of the power. Often the term transmission refers simply to the gearbox that uses gears and gear trains to provide speed and torque conversions from a rotating power source to another device[2]. The term transmission indicates all the necessary components for starting and moving a vehicle and mechanical machine. The main components that make up a transmission are : the transmission shaft, the gearbox, the clutch, the differential. A generic representation of gearbox of vehicle and its components, are shown in Fig.2.1.

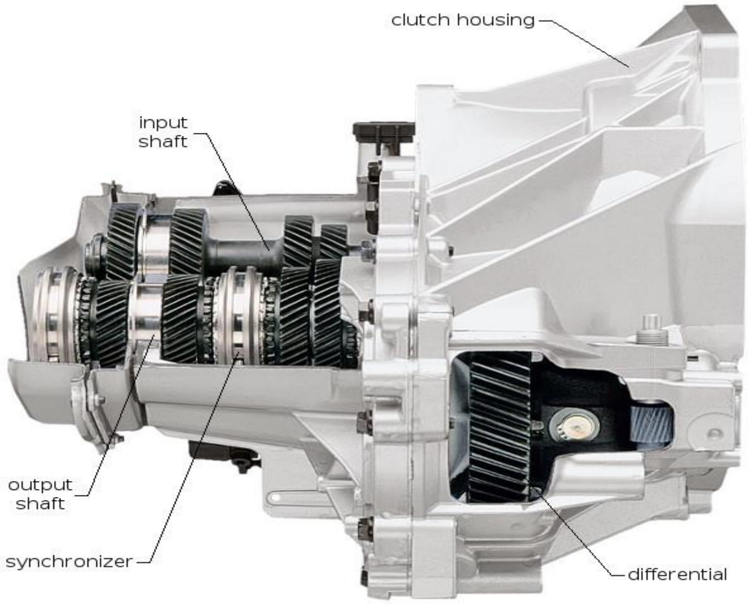

Fig.2.1 Mechanic Transmission[3]

The transmissions are widely used in motor vehicles where the use of the transmission has the objective of adapting the engine power to the torque of the driving wheels. The engines of the vehicles are characterized by a high rotation speed but having a high rotation speed is not appropriate for starting and stopping. The role of a transmission is mainly to reduce the speed provided by the engine to the speed required by the driving wheels. The transmission is characterized by the transmission ratios that allow to know the ratio in the variation of the speeds. There are transmissions that change over manually or automatically, there are single or multiple ratio transmissions. There are also hybrid configurations.

2.1.1 Transmission in Automotive

The need for a transmission in an automobile is a consequence of the characteristics of the internal combustion engine. Engines typically operate over a range of 600 to about 7000 rpm, while the car's wheels rotate between 0 rpm and around 1800 rpm[4]. The main shaft extends outside the case in both directions: the input shaft towards the engine, and the output shaft towards the rear axle. The main bearings support the shaft while a pilot bearing, at the point of split, holds the other shafts together. The gears and clutches ride on the main shaft, the gears being free to turn relative to the main shaft except, when engaged by the clutches.
The main vehicle transmission types are:

- Manual
- Semi-Automatic
- Automatic

2.1.1.1 Manual Transmissions

There are two principal kinds of manual transmission, the synchronized one and unsynchronized one. The unsynchronized transmissions need a manual synchronizing. The skill of the driver is important for a manual synchronizing where at each shift event he need to synchronize gear speeds. This kind of transmission is usually used in motorsport applications and heavy commercial vehicles. Most modern manual-transmission vehicles are fitted with a synchronized gear box, as shown in Fig.2.2.

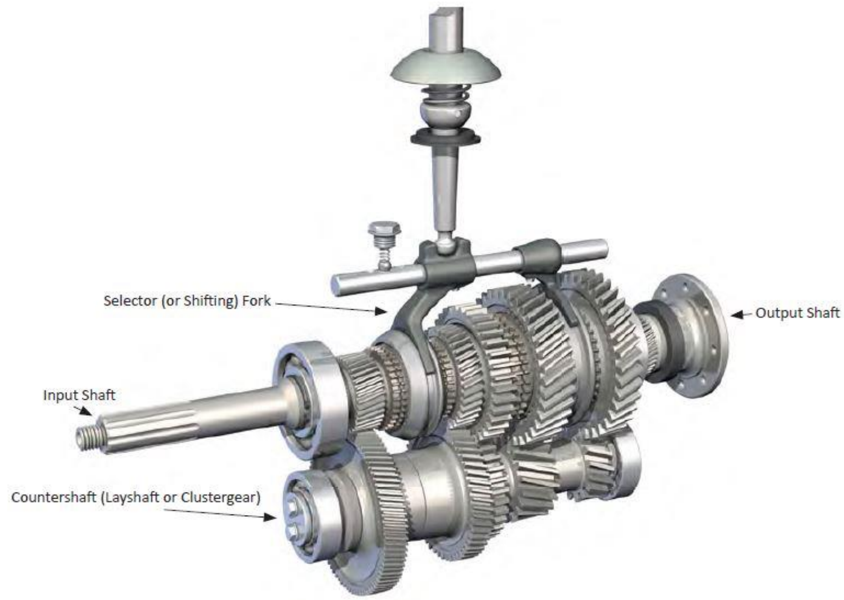

Fig.2.2 Manual Transmission[5]

Transmission gears are always in mesh and rotating, but gears on the principal shaft can freely rotate or be locked to the shaft. To lock the gears to the principal shaft it is necessary to use a collar on the shaft. This collar can slide sideways so that teeth on its inner surface bridge two circular rings with teeth on their outer circumference: one attached to the gear, one to the shaft hub. When the rings are bridged by the collar, the gear is rotationally locked to the shaft and determines the output speed of the transmission. The gearshift lever manages the collars and one collar may be permitted to lock only one gear at any one time. The operators must understand how to shift the transmission into and out of gear. A non-synchronous transmission is a form of transmission based on gears that do not use synchronizing mechanisms, then this transmission requires an understanding of gear range, torque, engine power, range selector, multi-functional clutch, and shifter functions.

2.1.1.2 Semi-Automatic Transmission

A semi-automatic transmission is a manual transmission with little actuators that do all the physical stuff that the driver would ordinarily be doing, as shown in Fig.2.3.

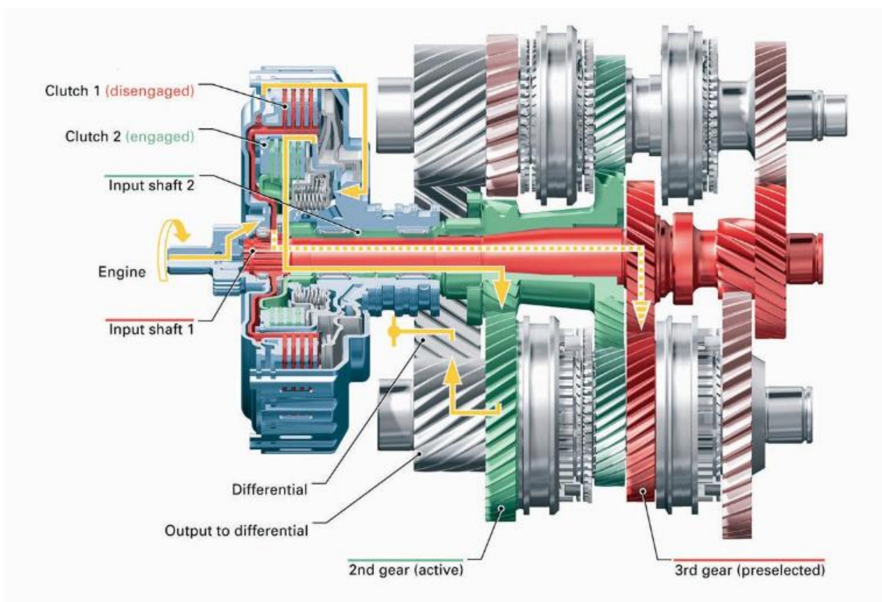

Fig.2.3 Semi-Automatic Transmission[6]

Often the transmission itself is a manual transmission that has had the additional semi-automatic components fitted to it. Actuators attached to the outside of the transmission take the place of a gear lever, selecting the appropriate gear for the driver. As the transmission itself is often just a standard manual gearbox, there will generally be two actuators to simulate both the up and down motions of a gear lever[7]. The clutch is controlled by a hydraulic pump, this pump simulates the pressing of the driver on the clutch pedal. All this system is managed by a control module that decides when to change gears. It is known that the semi-automatics have a better driving comfort compared to an automatic one, it also presenting many characteristic advantages of the manual ones. But the gear changes of the semi-automatic do not show a fluidity present instead in the automatics.

2.1.1.3 Automatic Transmission

An automatic transmission is characterized by the possibility of being able to automatically change the gear ratio of the vehicle in motion without the manual use of the driver. This type of transmission is mainly used in internal combustion vehicles characterized by a high speed of rotation and by important torque.. The most popular form found in automobiles is the hydraulic automatic transmission, as shown in Fig.2.4.

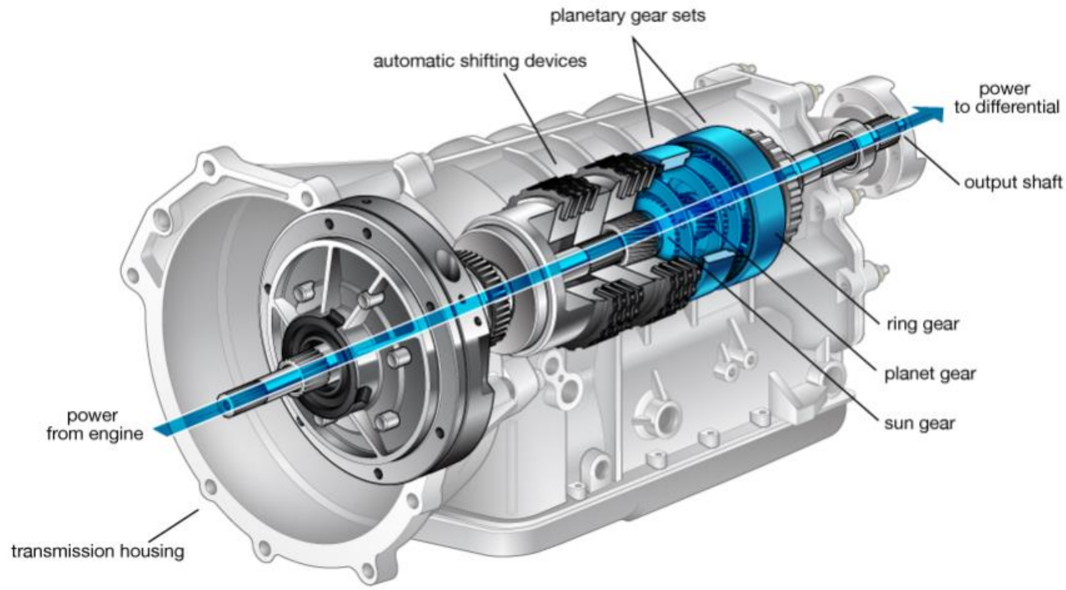

Fig.2.4 Automatic Transmission[8]

The characteristic of this system is using a fluid coupling and not using the system characterized by a friction clutch. Gear changes are also managed thanks to the action of locking and unlocking a planetary gear system in a hydraulic way. These systems are also defined by different gear ranges and are characterized by a safety system that can be defined as a parking pawl that blocks the transmission output shaft to prevent the vehicle from advancing or dipping. In the case of machines with limited speed ranges or fixed engine speeds they simply use a torque converter to provide variable engine transmission to the wheels.

2.2 Speed Reducer and Gearbox

The mechanical problem that is treated in the project concerns a gearbox for a thermal engine. The problems that are present in the gearbox, that is already in use and installed in vehicles, are to be avoided in the speed reducers that are used in electrfied vehicles.

2.3 Manufacturing Process

Generally, a mechanical component is characterized not only by its function in a mechanical system, but also by its material with which has been manufactured, by the mechanical manufacturing and heat treatment to which it has been subjected.

2.3.1 Machining

The main components of the gearbox are made of aluminum, steel or cast iron. A series of machining operations, performed with numerically controlled machines, allow to give them their final shape: turning, cutting, shaving, heat treatment, phosphating, grinding, lapping. The quality of the components is measured by means of control integrated into the machines Fig.2.7 and by statistical samples taken by the operators.

To ensure that te gearboxes operate properly, the teeth of the pinions and shafts must be adjusted to the nearest micron. To make micron toothings, the machining tools are sharpened and measured with maximum precision.

Fig.2.7 Numerical Control Machine[9]

2.3.2 Heat Treatment

After machining, all parts, except casings and housings, are subjected to heat treatment for carbonitriding operations. Carbonitriding is a metallurgical surface modification technique that is used to increase the surface hardness of a metal, thereby reducing wear. During the process, atoms of carbon and nitrogen diffuse interstitially into the metal, creating barriers to slip, increasing the hardness and modulus near the surface. Carbonitriding is often applied to inexpensive, easily machined low carbon steel to impart the surface properties of more expensive and difficult to work grades of steel.

Made in powerful furnaces Fig.2.8, this operation consists of treating the parts by heating them to 860 ° C to make them more resistant to mechanical stress and wear. This operation is essential to guarantee the durability of the gearbox.

Fig.2.8 Heat Treatment Furnace[9]

2.3.3 Gear Wheel Line Production

To produce the gear wheels, the cutting process is carried out through the hobbing process, and the grinding process using an abrasive wheel. Not all wheels are subjected to the same production process.
In order to study the harmonic phenomenon and understand its nature, the production cycle is as follows:

- Production of three pieces subjected to hobbing process, after heat treatment and finally to the grinding process.
- Production of a piece subjected to hobbing process, after shaving, heat treatment and finally to the grinding process.

It can therefore be observed that the difference between the two types of components produced is the presence or absence of the shaving process before heat treatment. It is important to note that the four gear wheels are produced on the same machine. It is necessary to study the production processes and understand if errors occur after the hobbing process or after the shaving or grinding process. Understand if the error is related to the machine or to other factors and searching for possible solutions. In order to carry out a detailed study of the possible causes, it is necessary to study the kinematic that manages the movement of the numerical control machines used in the production of helical wheel.

3

Manufacturing Process

Most modern gears are cut by a process known as generating cutting. During the cutting process the cutter and the gear blank are each rotated, as if they were a meshing gear pair. One of most common methods by which gears are generated is hobbing.

3.1 Hobbing

The hobbing system is characterized by a transmission system that aims to vary the speed and torque provided by the engine. The transmissions in this complex are mainly gear transmission and belt drive. The system, which is characterized by different shifting levels, allows to manage the speed of the machine according to the manufacturing needs. The strict speed and itinerary synchronization relationship of inline transmission chain is relied on transmission components having accurate transmission ratio, and therefore gear itself manufacturing error and assembly error on the accuracy of the final hob is the major role[10].

The relative movement of hob and workpiece is based on linear movement and rotational movement of each kinematic pair, including X linear motion, Z linear motion, Y linear motion, A, B and C rotary motion, which with machine bed, hob, piece together constitute hobbing physical structure Fig.3.1.

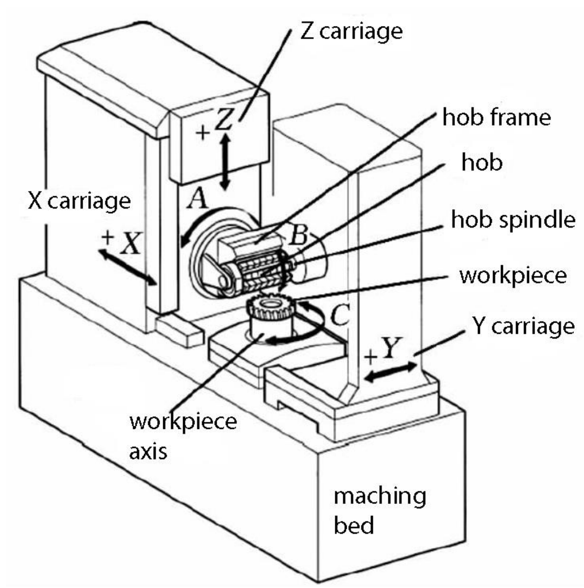

Fig.3.1 Hobbing Machine[10]

A typical hob Fig.3.2 has basically the same shape as a screw, with one or more threads, and each thread is cut by a few gashes, either at right angles to the thread, or parallel with the hob axis, so that cutting faces are formed.

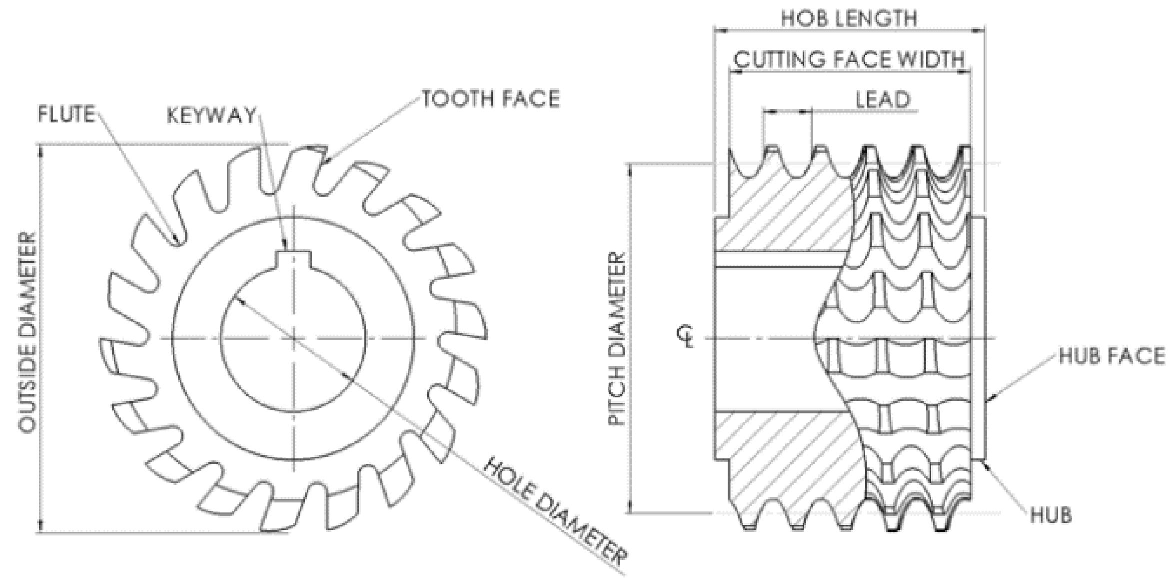

Fig.3.2 Hob[11]

When the hobbing system works, the hob is meshed to a work gear and during the meshing, the hob creates the teeth surfaces of an imaginary rack, as shown in Fig.3.3. It is necessary to have a enough profile of the rack tooth if we want to have a good involute profile of the work gear. It is also neccesary to have a good accuracy of the hob if we want a good result. It is important to consider also the contribute of hob mounting. To analyse the hobbing process normally we use concept of imaginary rack because the cutting process of the hob is similar to that of a rack cutter. The teeth of a hob must represent a helical rack moves in the direction of tangent to a pitch circle of a work gear with helix angle while the hob is rotated. It is necessary to incline the hob arbor axis at angle of the helix angle minus or plus the lead angle of the hob thread.

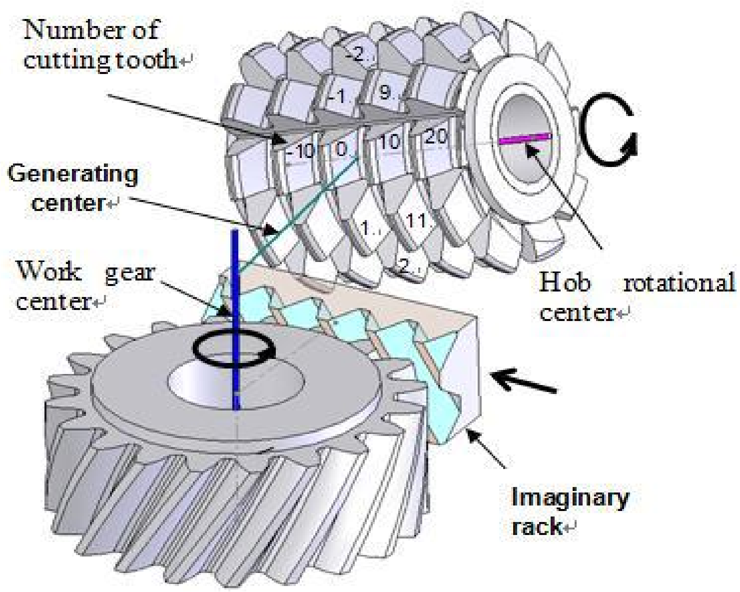

Fig.3.3 Imaginary rack, Generating center, Number of cutting tooth[12]

The hobbing process has two advantages over that of a rack cutter: in both the axial and the tangential directions the motions of the cutting faces are continuous, so there is not necessary to move the hob back after that, one or two teeth are cut (as in the rack cutting system) and the cutting action is obtained without any reciprocating motion of the hob and the hob is fed slowly in the direction parallel to the gear axis. As we said previously, each hob's cutting face simulates a tooth of the rack cutter, then the hob is tipped over by an angle called swivel angle Fig.3.4, for meet the gear blank and the cutting faces at the same angle of the rack cutter.

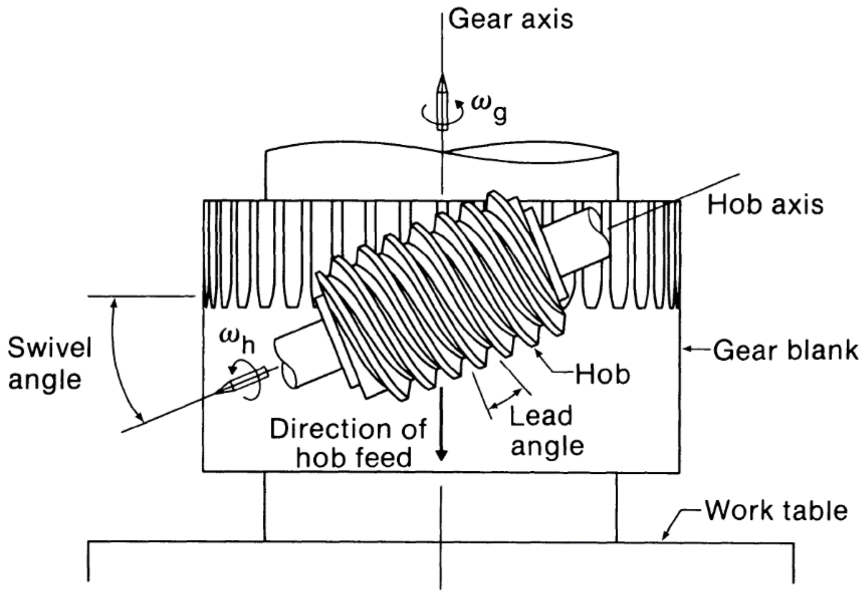

Fig.3.4 Direction of hob feed[13]

The normal section is the one where the hob thread stays perpendicular to the direction of the thread, and there are differents kind of hobs which are designed to have the threads shaped in the normal section in the same way of the teeth of a rack cutter. If we want to have the same shape of the cutting faces like the one of the teeth's rack cutter, we need to have the gashes of the hob perpendicullary to the direction of the threads. During the hobbing process, the rack cutting system is simulated because the cutting pitch circle in the gear blank is the same with its standrard pitch circle[13]. For the tooth thickness we need to pay attention to two factors: the thickness of the hob and the depth to which the hob is fed into the gear blank. During the hobbing process we cannot confirm that this process is exactly like a rack cutting system because there are some errors, but these errors are so small.

3.1.1 Manufacturing defects

Although we plan a precise modeling of the machining processes, such as cutting and grinding processes, defects are unavoidable. The main manufacturing defects are due to errors related to assembly, to the kinematics of the cutting or grinding machine and machine for making the tool. These defects therefore induce disturbances on the theoretical cutting path. By analyzing the defects present in the wheel tooth of a helical gear, the main origins of the defects are:

- Pinion assembly fault
- Defect of assembly of the cutting tool
- Operating fault of the cutting machine
- Operating fault of the grinding machine

Analytically we can define any manufacturing defect by characterizing it through a displacement torsore. In general, we can call with **ε** the defect and with $\boldsymbol{\tau_\varepsilon}$ the corresponding displacement torsore whose center is called **Oε** and whose base is defined through the unit vectors (**$\mathbf{n_{\varepsilon x}}$, $\mathbf{n_{\varepsilon y}}$, $\mathbf{n_{\varepsilon z}}$).**

The displacement torsor is therefore defined as follows[14]:

$$\tau_\varepsilon = \begin{cases} \vec{\omega}_\varepsilon^{R_\varepsilon} = Rx.\vec{n}_{\varepsilon x} + Ry.\vec{n}_{\varepsilon y} + Rz.\vec{n}\varepsilon z \\ \vec{\delta}_\varepsilon^{R_\varepsilon}(O_\varepsilon) = dx.\vec{n}_{\varepsilon x} + dy.\vec{n}_{\varepsilon y} + dz.\vec{n}\varepsilon z \end{cases}$$

Considering then a generic point on the surface of the tooth and defined the vector $\vec{\boldsymbol{p}}_{\boldsymbol{O_\varepsilon P}}^{\boldsymbol{R_\varepsilon}}$ as the vector that joins the center $\mathbf{O_\varepsilon}$ with the generic point **P**, we can define the displacement of this point as[14]:

$$\vec{\delta}_{\varepsilon}^{R_\varepsilon}(P) = \vec{\delta}_{\varepsilon}^{R_\varepsilon}(O_\varepsilon) + \vec{\omega}_{\varepsilon}^{R_\varepsilon} \wedge \vec{p}_{O_\varepsilon P}^{R_\varepsilon} \qquad (3.1)$$

When we have different manufacturing defects, we need to study and analyze the combination of different effects. It is necessary to suppose the geometric defects created during the cutting process with dimensions much lower than the dimensions of the tooth, we will consider it with orders of magnitude of the micron. After analyzing any manufacturing defect, the resulting geometric defect that will be obtained will be given by the algebraic sum of all the individual defects determined for each manufacturing defect. Before doing this, the various manufacturing defects must be modeled analytically and related to the same reference system.

3.1.1.1 Defects of the inaccuracy of the cutting machine.

Mainly it is possible to divide the defects caused by the imprecision of the hobbing machine as follows:

- The defects related to the geometry of the machine, to the static defects of misalignment of the different axes between them.
- The defects related to the movement of the machine, then the kinematic problems of the machine.

To verify the absence of misalignment errors of the machine axes, first must choose one of the axes as the reference axis respect to which the measurements is made. It is usually recommended to choose as a reference axis, an axis that is common for the different types of cutting machines, for example the axis of rotation of the workpiece platform where the pinion to be cut is installed, and we can refer to the standard NF-ISO 6545. The standard authorizes, for a 500 mm machine advancement stroke, misalignment defects of 3e-5 rad, therefore relatively low values. The same study must also be carried out for the rotation axis of the machine, where the cutting tool is positioned. Also, for the hob it is fundamental that its axis of rotation is oriented according to the theoretical orientation. Generally, to mesure the misalignment of hob are used two sensors on both sides Fig.3.5.

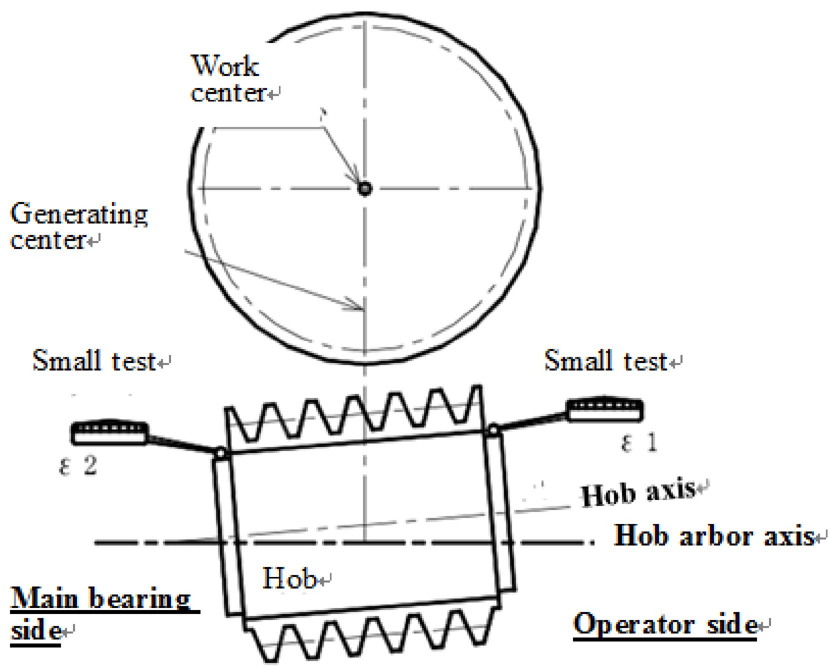

Fig.3.5 Axis Misalignment[12]

Another type of error very common in mechanical system, is the transmission error. This error is the rotation delay between driving and driven gear caused by the disturbances of inevitable factors such as elastic deformation, manufacturing error, alignment error in assembly[15]. Defining $\boldsymbol{\theta_1}$ and $\mathbf{z_1}$, respectively the angular position and the number of teeth of the driving wheel and $\boldsymbol{\theta_2}$ and $\mathbf{z_2}$, respectively the angular position and the number of teeth of the driven wheel, the transmission error is defined as follows[16]:

$$EdT = \theta_2 - \frac{z_1}{z_2}\,\theta_1 \qquad (3.2)$$

It is also possible to define a generic equation to determine the transmission error caused by eccentricity of a pinion of a cinematic chain as follows[14]:

$$EdT(i) = \frac{e(i)}{r_b(i-1)\,Z_{eq}(i-1)}\,sin(\theta_{ei} + Z_{eq}(i)\,\theta_p) \qquad (3.3)$$

Where:

$e(i)$	eccentricity of the pinion (i)
θ_{ei}	angular phase of the eccentricity according to the pinion reference (i)
$r_b(i-1)$	base radius of the pinion (i-1)
$Z_{eq}(i-1)$	speed ratio between the pinion (i-1) and the workpiece platform on which it is installed
$Z_{eq}(i)$	speed ratio between the pinion (i) and the workpiece platform on which it is installed
θ_p	angular position of the workpiece platform

3.1.1.2 Defects caused by inaccurate assembly of the pinion and cutting tool

The assembly of the pinion and cutting tool can most often present deviations from the theoretical assembly. The inaccuracy of the assembly can be given by the linear combination of one or more deviations simultaneously. Taking as an example the axis of rotation of the pinion: it can have an eccentricity, so it remains parallel to the theoretical axis, but it is shifted. The same axis, now shifted, can also have an angular deviation. The same problem can be found in the assembly of the tool on the cutting machine, even for the tool rotation axis we can have the displacment of the theoretical axis and an oscillation. For both cases it is possible to calculate the error through a torsore that considers both phenomenons, according to the local reference system of the pinion or hob.

Fig.3.6 shows the presence of eccentricity represented by the displacements Δx, Δy, Δz and the angular deviations represented by the oscillations $\Delta\theta x$, $\Delta\theta y$, $\Delta\theta z$, of a generic cylindrical structure, which can rappresents the pinion or the hob.

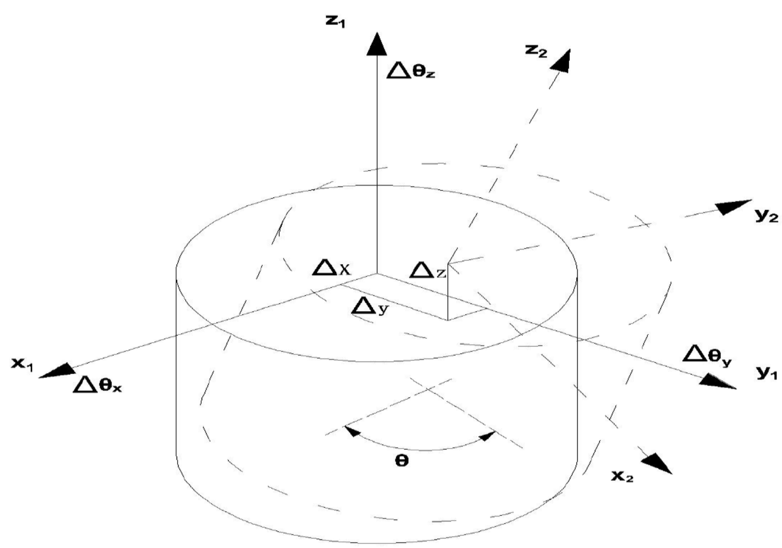

Fig.3.6 Linear and Aangular Deviations[10]

3.1.1.3 Defects generated by the inaccurate grinding of the cutting tool

Grinding is an abrasive machining process that uses a grinding wheel as tool. The grinding is a true metal-cutting process. Each grain of abrasive functions as a microscopic single point cutting edge. Grinding is used to finish workpieces that must show high surface quality and high accuracy of shape and dimension. As the accuracy in dimensions in grinding is of the order of 0.000025 mm, in most applications it tends to be a finishing operation and removes comparatively little metal, about 0.25 to 0.50 mm depth[17]. However, there are some roughing applications in which grinding removes high volumes of metal quite rapidly. The grinding operation can concern both the hob and the wheel.

The tool used to perform the grinding operation is the grinding wheel. This is an expendable wheel used for various grinding and abrasive machining operations. It is generally made from a matrix of coarse abrasive particles, they are before pressed and then bonded together to form a solid, circular shape and various profiles. Grinding wheels may also be made from a solid steel or aluminium disc with particles bonded to the surface. One example among many others are shown in Fig.3.8.

Fig.3.8 One example of Grinding Tools[18]

If the cutter grinding operation is not carried out correctly, this error will affect the cutting operation that will be carried out subsequently, thus obtaining low quality gears. The hob error that is present during the grinding processis called hob rake error. The rake error is described as the tooth face tolerance relative to the centerline of the hob which is measured from the full cutting depth to the outer diameter of the hob tooth[19]. The tooth face of a hob with zero rake design extends on a theoretical line through the center of the hob as shown in Fig.3.9.

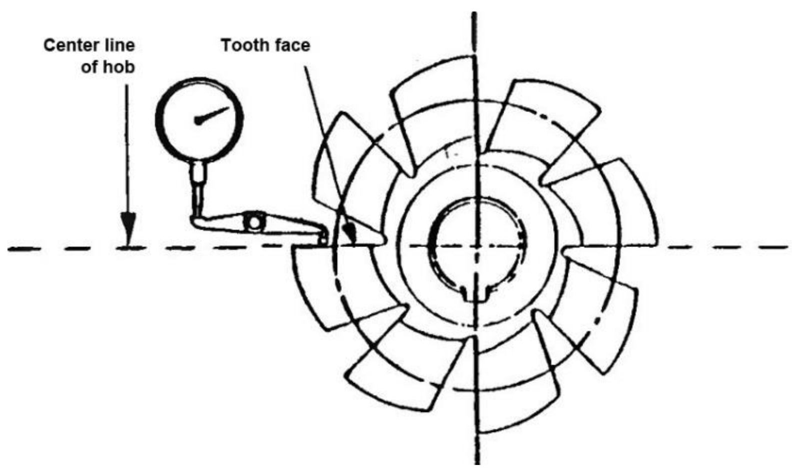

Fig.3.9 Zero Rake Error[19]

When the hob is grinding, the original rake angle of the tooth must be maintained whether it was designed with a positive, radial or negative rake angle. If an excessive stock has been removed from the lower part of the hob tooth face the depth of the tooth has increased and we have a positive rake error Fig.3.10. If there is a decrease of pressure angle, this produces an incorrect involute profile when generating a gear. The gear tooth with a plus condition toward the tip is produced by a decreased of pressure angle. This type of condition may cause gear noise and premature failure. If the grinding or hobbing wheel removes excessive stock from the upper portion of the hob tooth face we have then a negative rake error. This meaning that the depth of the hob tooth is deceased, but the pressure angle has increased. Rake error is usually caused by an incorrectly positioned of grinding or hobbing wheel due for example for an incorrect mounting, or an incorrectly dressed wheel. If we want to to correct this kind of error, it possible to repositioning the principal axe of grinding or hobbing wheel on the hob grinder.

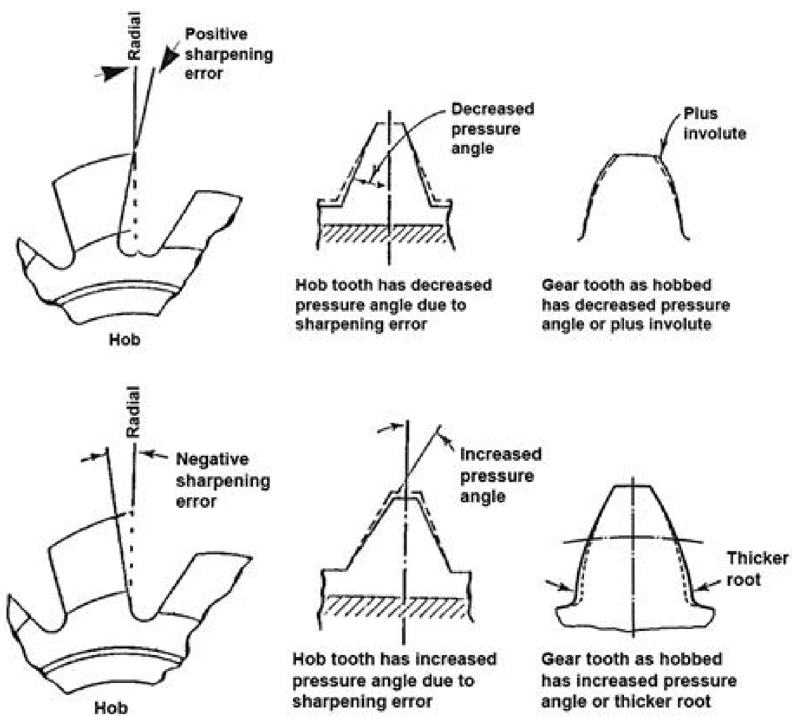

Fig3.10 Positive and Negative Rake Error[19]

4
Gear Whine Noise

When developing a mechanical transmission one important characteristic of the transmission is how much tonal noise and vibrations it generates. The vibrations causing the gear whine noise is generated in the gear contacts of the transmission and propagate through the shafts and bearings to the housing, where they become airborne. In electrical vehicle the absence of a loud combustion engine makes the gear whine noise more distinct and easily perceived by the human ear. There are many types of different noises associated with gears, but one of the more distinct noises is the gear whine noise. This noise is emitted from gears that are in mesh and the sound is characterized as vibrations with frequencies same as the gear mesh frequency and its multiples.

The noise exhibits a periodic behaviour and it is therefore perceived as a tonal noise. It is therefore an important factor when reducing the noise level of transmissions since the human ear is more sensitive to tonal noises, compared to noises with more random characteristics. Because the acoustic pressure, due to gear whine noise, is not necessarily proportional to the engine speed the unexpected noise and therefore the undesirable acoustic phenomena due to the power system could be high in any engine running condition[20]. For that reason, gear whine noise represents an important problem to solve or to reduce or to manage at least in an appropriate way.

Many factors influence the vibro-acoustic emissions, mainly they are:

- Transmission error
- Variation of meshing stiffness
- Dynamical forces of meshing
- Friction forces
- Detention of air and lubricant between the teeth

The mainly cause of generation of the noise in the mechanical transmission are the forces. When we have an important variation of forces, this causes the vibration of different components present in the transmission. These forces generally change in amplitude, direction or position and this changment is caused by surfacing errors. The vibrations are then transmitted to the shafts through the bearings to the housing, when the housing is excited the noise is propagated to the vehicle and the noise is heard from the driver. Vibrations are also transferred through the housing mountings where they can excite other external components, such as parts of the compartment in a vehicle.

The flow chart below shows the noise path from the source to the external environment.

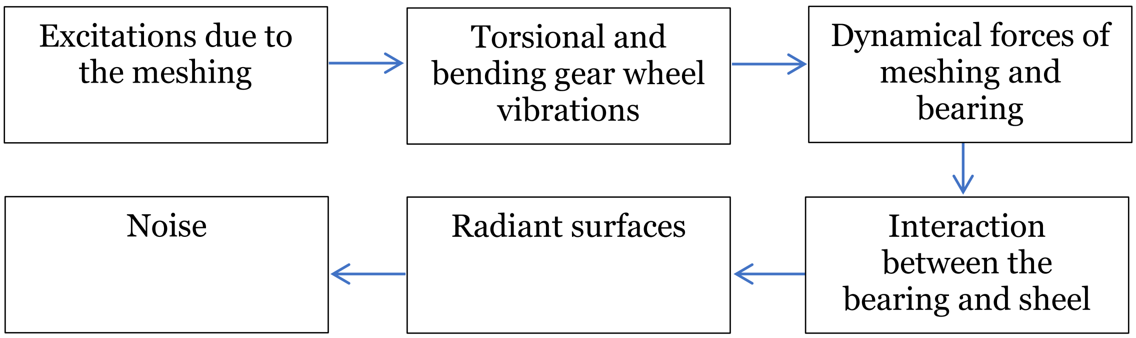

4.1 Description of gear profile measuring machine

To inspect the presence of surfacing profile errors on the gear wheel, a specific machine is used to control and check cylindrical gears, pinion cutters and shaving cutters, worms and worm wheels, hobs. Specifcly this machine wants to research different types of deviations in dimension, location and position of symmetrical pieces. Further applications include also some cams and camshaft measurement and rotor measurement. Klingelnberg measuring centres today are one of the most important measuring center of this kind of machines and engineering applications, they represent one of most important brands in different sectors: automotive, commercial vehicle industries, aerospace, aeronautical engineering industries.

This allows the following measurement tasks to be fully automated in a single setup:

- Gear measurement
- Optical measurement
- General coordinate measurement
- Form and position measurement
- Roughness measurement
- Contour measurement

Fig.4.2 shows the trajectory effected by the head of the measuring machine for obtaining lead line, pitch, concentricity and profile the tool used for the helical gear profile measurement.

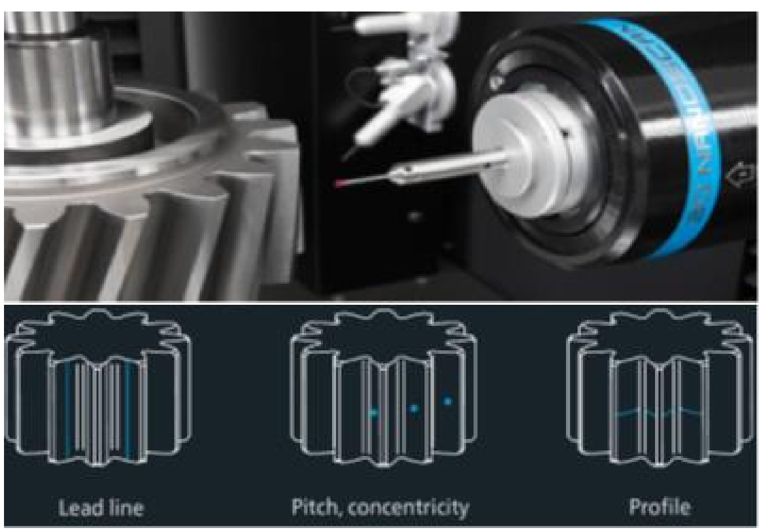

Fig.4.2 Measurement[21]

For an excellent precision measuring centre, it is necessary to consider the accuracy, reproducibility and durable rotary table. Firstly, it is necessary to configure the machine and guarantee the concentricy seating of the workpiece. If the concentricity is checked, with the combination of three linear measuring axes (tangential, radial and vertical), the precision measuring centres is able to trace and control the functional surfaces of gearing and general mechanical components. This guarantees the maximum measuring ratio of accuracy and reproducibility.

This type of measuring centres used to control the quality of the component normally are characterized by a heavy-duty, stable beds and guide system. The bearings and guides are backlash-free at the measuring axes, this kind of property is the basis for the high basic mechanical technologic of measuring centres. The integrated 3D tracer head enables both discrete-point tracing and scanning and continuos measuring.

4.2 Influence of tooth surface undulation on noise

To ensure vibration quality and quiet operation, gears are manufactured so that their geometry is as close as possible to their design. In practice, however, there are always irregularities during the manufacturing process that lead to various kinds of gear errors and resultant vibration and noise problems. Usually gear vibration is mainly observed at the fundamental tooth meshing frequency and its harmonics. However, it is known that when gear errors exist, many other frequency components are also observed at the same time. Common errors of every gear tooth lead to vibration at meshing frequencies as well as the variation of tooth stiffness during meshing. Pitch error and the other fluctuations from common tooth shape bring about vibrations at low frequency bands and sidebands surrounding meshing components[22].

Vibration attributed to gear local defects such as crack or nick is observed as the occurrence of an impulsive wave in time domain or a lot of comb spectra in wide frequency range[23].

There are also different kinds of errors that cause vibrations at the one order of frequency that is not part of nominal of meshing frequency. It is so difficult to find the real reason of this kind of vibrations because the frequency of these vibrations is not related directly to some specified geometries or form of the gear. The vibration source cannot be detected by ordinary tooth profile measurement equipment, and for this reason, this vibration component is usually called ghost noise. It is known that ghost noise is created by a periodic cyclic undulation on the surface of a gear tooth continuing from one tooth to the next. The source of this undulation can be traced to the irregularity in the process of generation.

The two types of undulation present during the manufacturing process are:

- Profile undulation
- Helix undulation

4.2.1 Profile undulations

The profile undulations are caused by errors present in the real profile of the wheel, then the real profile of the wheel is different from the theoretical profile. The profile undulation can be generated during the manufacturing process or by wear and deterioration of the wheel during the gear meshing. ISO 1328 defines the profile error as the amount by which a measured profile deviates from the design profile. We have mainly three different kind of profile error: total profile deviation, profile form deviation and profile slope deviation.

- Total profile deviation F_{α}

  Distance between two facsimiles of the design profile which enclose the measured profile over the profile evaluation range. The facsimiles of the design profile are kept parallel to the design profile.

- Profile form deviation $f_{f\alpha}$

  Distance between two facsimiles of the mean profile line which enclose the measured profile over the profile evaluation range. The facsimiles of the mean profile line are kept parallel to the mean profile line.

- Profile slope deviation $f_{H\alpha}$

  Distance between two facsimiles of the design profile which intersect the extrapolated mean profile line at the profile control diameter and the tip diameter.

The mean profile line represents the shape of the design profile aligned with the measured trace over the profile evaluation range. The profile evaluation range represents the section of the measured profile starting at the profile control diameter and ending at 95 % of the length to the tip form diameter[24].

4.2.2 Helix undulations

The helix undulations are defined by ISO 1328 as amount by which a measured helix deviates from the design helix. The helice deviation are measured in the direction of base cylinder tangents, in the apparent plane.
We have mainly three different kind of helix error: total helix deviation, helix form deviation and helix slope deviation.

- Total helix deviation $\boldsymbol{F_\beta}$

Distance between two facsimiles of the design helix which enclose the measured helix over the helix evaluation range. The facsimiles of the design helix are kept parallel to the design helix.

- Helix form deviation $\mathbf{f_{f\beta}}$

Distance between two facsimiles of the mean helix line which enclose the measured helix over the helix evaluation range. The facsimiles of the mean helix line are kept parallel to the mean helix line.

- Helix slope deviation $\mathbf{f_{H\beta}}$

Distance between two facsimiles of the design helix which intersect the extrapolated mean helix line at the end points of the facewidth, b

The mean helix line represents the shape of the design helix aligned with the measured. The helix evaluation range is the flank area between the end faces or, if present, the start of end chamfers, rounds, or other modification intended to exclude that portion of the tooth from engagement, that is, unless otherwise specified, shortened in the axial direction at each end by the smaller of 5 % of the facewidth or the length equal to one module[24].

Fig.4.4 shows profile and helix deviations with unmodified involute.

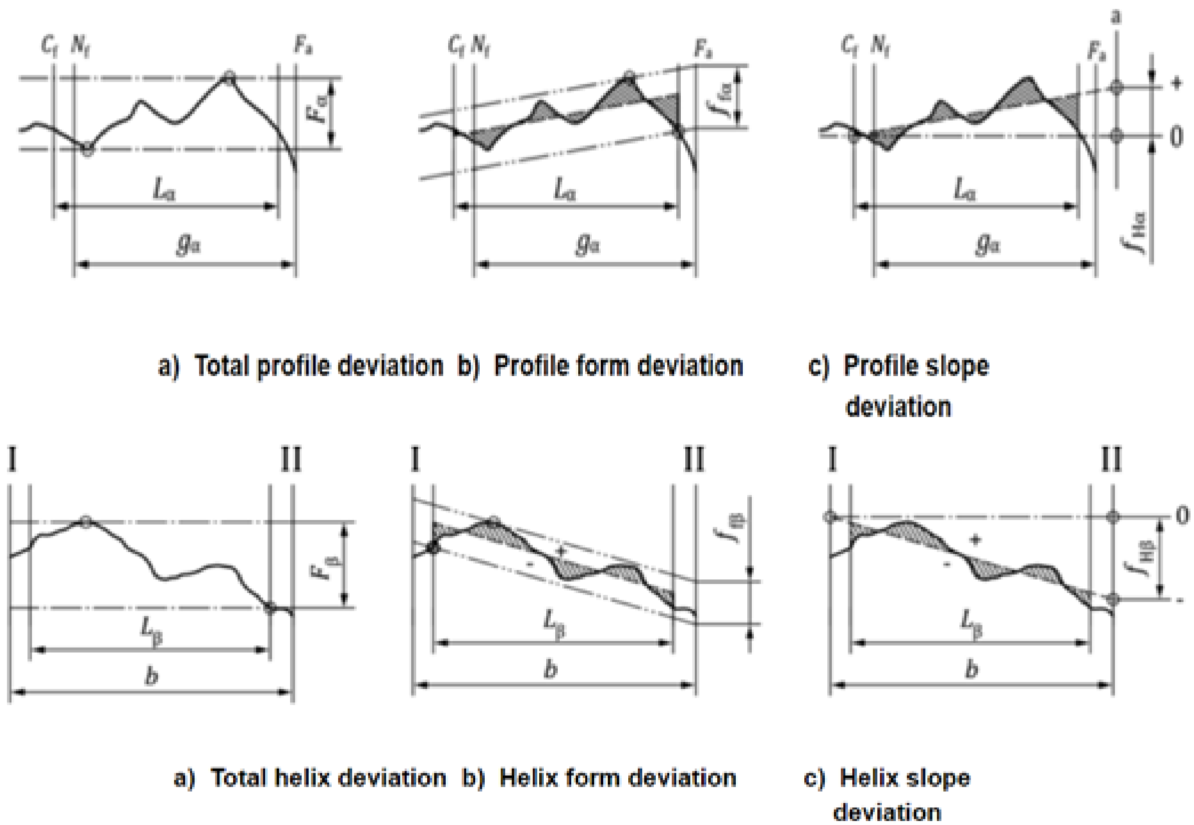

Fig.4.4 Profile and Helix modification[24]

Where:

measured profile

facsimile of design profile

mean profile line

facsimile of mean profile line

F_a	tip form
a	tip
C_f	profile control
N_f	start of active profile
L_α	profile evaluation length
g_α	length of path of contact
L_β	helix evaluation length
b	facewidth

4.2.3 Generation of undulations

To understand the generation of undulations, the kinematic relation in the grinding machine MAAG it has been treated in the report of Georges Henriot[25], he associated the origin of undulation to the workout platform from an error of the worm wheel. This error is therefore generated by the rotation frequency of the screw. One of most common error related to the screw is the eccentricity error. This causes an angular deviation of the screw respect to its theoretical position. This angular deviation is a sine wave with amplitude A Fig.4.5.

$$A = x_0 tg(\alpha_0) \qquad (4.1)$$

Where:

X_0 eccentricity error per turn

α_0 pression angle

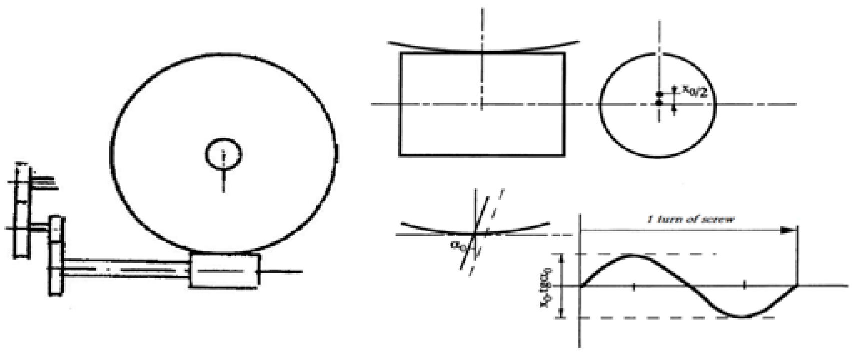

Fig.4.5 Eccentricity error of worm wheel[25]

The tool or grinding wheel removes too much material or less if this error is present, then the helical wheel has some ripples on the profile.
It is possible to represent the section of the teeth as an undulation with wavelength λ_β.

$$\lambda_\beta = \frac{\pi\, d}{Z_0 tg(\beta)} \qquad (4.2)$$

Where:

d primitive diameter

Z_0 number of teeth

β helix angle

When the wheel moves it removes the metal following some undulations having the angle of inclination of the generators δ Fig.4.6.

$$tg(\delta) = tg(\beta)sin(\alpha_n) \qquad (4.3)$$

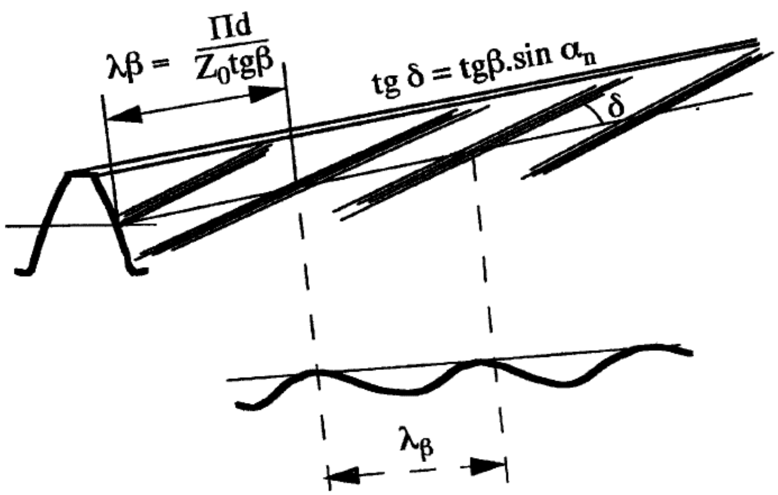

Fig.4.6 Undulation[25]

If we consider the meshing between the wheel and the pinion, the meshing meets different ripples during the work. This generates an angular deviation of the wheel and during the meshing there will be a noise which frequency will be:

$$\frac{n\,Z_0}{60}\ Hz$$

Where:

n turn · min^{-1} of the wheel

5

Method

In the previous chapters, it was highlighted that in mechanical transmission system, gear pairs are widely used in automotive industries because of its accurate transmission ratio and good reliability. Noise is created during the engagement of gear pairs system and the vibration comes down to excitation of gear transmission error. Many literatures have revealed that transmission error is the main parameter that affects the performance and quality of transmission of gear pairs, especially for noise vibration harshness performance of vehicle.

We decided to introduce some profile modification of the gear pairs to try to detect the reason and the source of the gear whine noise. This kind of method is already adopted by other researchers to study this phenomenon.
For exemple, modifying the tooth profile it is possible to decrease the interference during the meshing and compensate teeth deflection under load without sacrificing the tooth strength. Another type of error that can be decreased by tooth modification is the transmission error.

5.1 programming software

Before to proceed with kinematic study of manufacturing machines, it is necessary to analyze different possible ways for project development. It is possible to adopt two different ways of resolution: MATLAB or CATIA V5. Using programming codes to design gear models is much simpler compared to professional drawing software (Catia V5, SolidWorks, AutoCAD), especially for designing tooth profile modification. If we want to proceed by first way, it is necessary to begin with theoretical kinematics study of manufacturing machine, analyzing different equations that establish the working trajectories of the machine, then implemented these equations on MATLAB numerical calculation program to generate the wheel surface. The second way is to generate the helical wheel using CATIA V5 software. It is therefore necessary to analyze the advantages and disadvantages of two software and then choose which one is best to develop the project. In this section we will describe the characteristics of these methods to solve the problem.

5.1.1 Matlab

MATLAB is the acronym of matrix laboratory. It is a multi-paradigm numerical computing environment and proprietary programming language developed by MathWorks. MATLAB allows matrix manipulations, plotting of functions and data, implementation of algorithms, creation of user interfaces, and interfacing with programs written in other languages, for example:

C, C++, C#, Java, Fortran and Python[26]. MATLAB comes with feature that allows you to design a graphic user interface, which can provide a convenient way to the users who can interact with the electronic device without knowing the programming code, but this is possible if a mechanical design is not required. In our case, we want to design an engagement between a hob and a helical wheel.

To design gear models in MATLAB, the first step is to find out the functions and the relationships of all the curves of the gear from mathematic and geometric point of view, and then use proper MATLAB codes and functions to program it. To draw the gear models by MATLAB codes is difficult at the beginning. Firstly, all the functions and relationships of gear curves should be found out from mathematic and geometric point of view. Then, we must to study all equations to design the gear and the relationship between the gear and the hob during the engagement and before it. Secondly, all the curves of gear models are made up of a series of nodes in matrix form, so how to handle with matrix operation like matrix addition, matrix rotation should be learnt. Thirdly, proper MATLAB programming languages and functions should be used. MATLAB Graphic User Interface is designed at last, which gathers all the programming codes in a single file. In the Graphic User Interface, we can obtain different kinds of gear models and draw then adding some tooth profile modifications. If we want we can also study the helical wheel with CATIA using the design of the wheel made on MATLAB, because it is possible to import the MATLAB data point file in CATIA, then it is possible to open the modelling the wheel by CATIA functions.

5.1.2 CATIA V5

CATIA is the acronym of computer-aided three-dimensional interactive application. It is a multi-platform software suite for computer-aided design (CAD), computer-aided manufacturing (CAM), computer-aided engineering (CAE), PLM and 3D, developed by the French company Dassault Systèmes. CATIA V5 is a complex engineering design software used, among many others, in parametric 3D modeling, surface modeling and cinematic and structural simulations. Commonly referred to as a 3D Product Lifecycle Management software suite, CATIA supports multiple stages of product development (CAx), including conceptualization, design (CAD), engineering (CAE) and manufacturing (CAM). CATIA facilitates collaborative engineering across disciplines around its 3DEXPERIENCE platform, including surfacing & shape design, electrical, fluid and electronic systems design, mechanical engineering and systems engineering[27].

CATIA facilitates the design of electronic, electrical, and distributed systems such as fluid and heating, ventilation, and air conditioning systems, all the way to the production of documentation for manufacturing. It contains comprehensive libraries for standard parts and has the possibility to create user defined libraries for repetitive content. Helical gears are parametric parts and the geometry of a helical gear is controlled by known parameters. In CATIA from specific geometric data on helical gears, the source solid is created as base for the digital 3D gears family. There are many methods available for developing profiles of gear and spline teeth. Most of the techniques are inaccurate because they use only an approximation of the involute curve profile. In addition, the involute curve by equation technique allows using either Cartesian in terms of X, Y, and Z or cylindrical coordinate systems to create the involute curve profile. Since gear geometry is controlled by a few basic parameters, a generic gear can be designed by three common parameters namely the pressure angle α, the module m, and the number of teeth Z. CATIA V5 uses these parameters, in combination with its features to generate the geometry of the helical gear and all essential information to create the model[28].

Gear development using parametric method means that the dimensions control the shape and size of the gear. The gear should have the ability to be modified, and yet remain in a way that retains the original design intent. By storing the relationships between the various features of the design and treating these relationships like mathematical equations, it allows any element of the model to be changed automatically and regenerate the new model. If we have a parametric model, we can have a degree of design flexible and we can also allow curved surfaces to be rationalized and building components of highly complex. Geometric forms so they can be built economically and efficiently. Since models are developed from the template the time consumed for gear modeling each time based on the parameters assigned is reduced. In fact, few entries in the input screen develops the gear in no time. Cost of development of the model is lesser because of time. The human fatigue is also very less.

In the table below the advantages and disadvantages of MATLAB and CATIA V5 are sown.

	ADVANTAGES	DISADVANTAGES
MATLAB	- Accurate system - creating specific uncorrected and corrected gear profiles - preparing the teeth profile individually - an expert user is not required to use the software	- Accurate study of machine's kinematics to create the code - long time to design - laborious method
CATIA V5	- Study of machine's kinematics is not required - no code is written - low time to design	- inaccurate system - creating ordinary representation of the gear - parametric method - expert user is required to use the software

The MATLAB software is chosen to design the helical gear. MATLAB is chosen because it offers accurate results without approximations provided by the software. Moreover, the accurate study carried out at the Polytechnic allowed me to have the requisites to analyze the problem from a kinematic point of view and the accurate knowledge of my supervisors about gearbox, manufacturing process and their experience allowed us to decide MATLAB as a programming software.

5.2 Modeling of the cutting process.

The working principle of the cutting process through the cutter It can be traced to a gear between helical wheels. The tooth of the pinion is generated by the teeth of the cutter, the gear is defined without clearance and the cutting takes place simultaneously on the two sides of the pinion. To simulate the cutting process, it is necessary to deepen the kinematics that regulate the relative movements of the two components: pinion and cutter. After analysing the relative position of the rotation axes of the pinion and the milling cutter, it is possible to proceed to obtain the contact points during the meshing and fifth the theoretical cutting points of the pinion tooth. Having obtained the theoretical cutting points on the toothing of the pinion, a comparison between the theoretical and real points can be made. Before proceeding with the modeling, it is necessary to define the pinion geometrically, defining the reference system.

5.2.1 Helical pinion reference system

Two local reference systems have been defined for the two components, respectively. The local reference system integral with the pinion during the cutting process is called **Rp** Fig.5.1. The theoretical rotation axis, therefore, without errors, is **Zp**. The origin of the reference system is given by the intersection of the **Zp** axis and the lower face of the pinion perpendicular to this axis. The **Xp** axis defines the symmetry axis of the first tooth of the toothing on the plane whose Zp coordinate is zero. The third axis is **Yp**. The three axes are oriented according to the unit vectors respectively $\mathbf{n}_{xp}$,$\mathbf{n}_{yp}$,$\mathbf{n}_{zp}$.

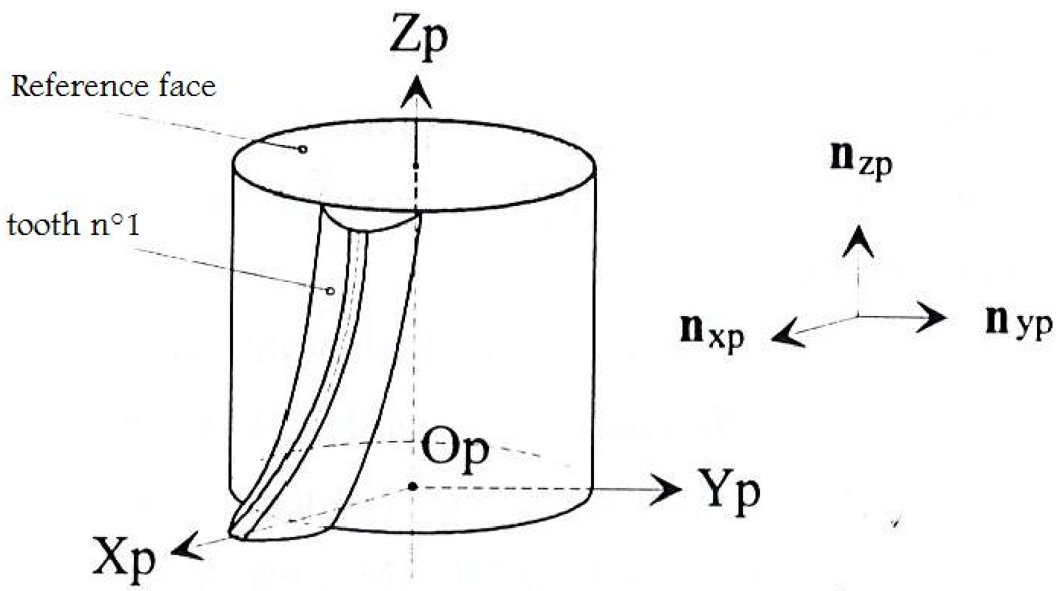

Fig.5.1 Pinion reference system[14]

The numbering of the teeth is performed in ascending order from the Xp axis to the Yp axis Fig.5.2.

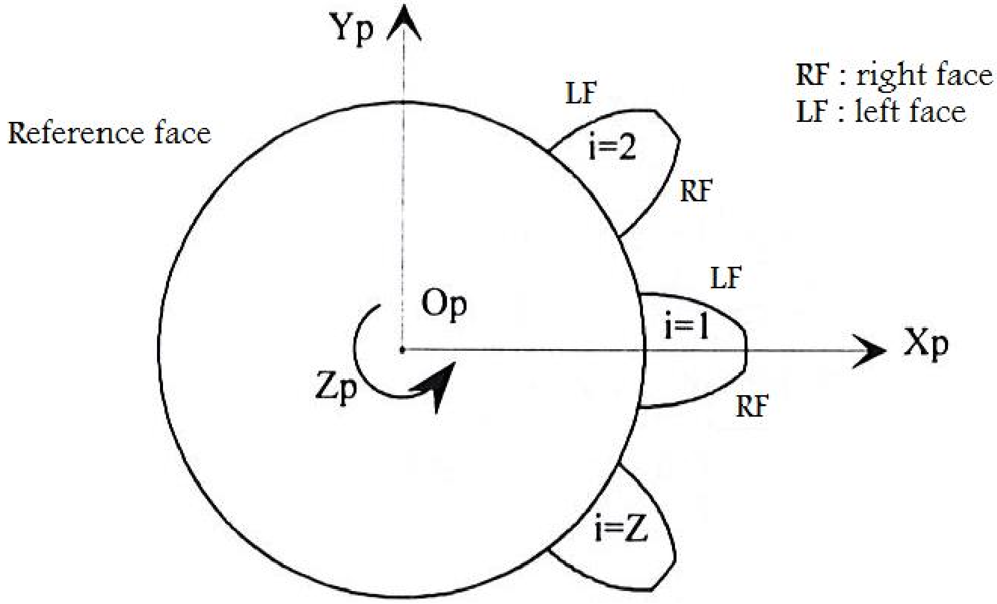

Fig.5.2 Numbering of pinion teeth14

To define a point belonging to the helical toothing, the apparent plane of the tooth is taken as the reference plane. The apparent plane is defined by the Xp and Yp axes. The apparent plane constantly has the perpendicular Zp axis. It is possible to draw a tooth thanks to the involute of the basic circle of the toothed wheel. Assuming that point A is on the tooth -thes i, a coordinate zm of the Zp axis and belongs to a cylinder of radius rm whose axis is Zp, this point is defined by three cylindrical coordinates: **$A(r_A,\theta_{iA},z_A)$.** Fig.5.3 shows the apparent plane of the helical tooth and its goniometric references.

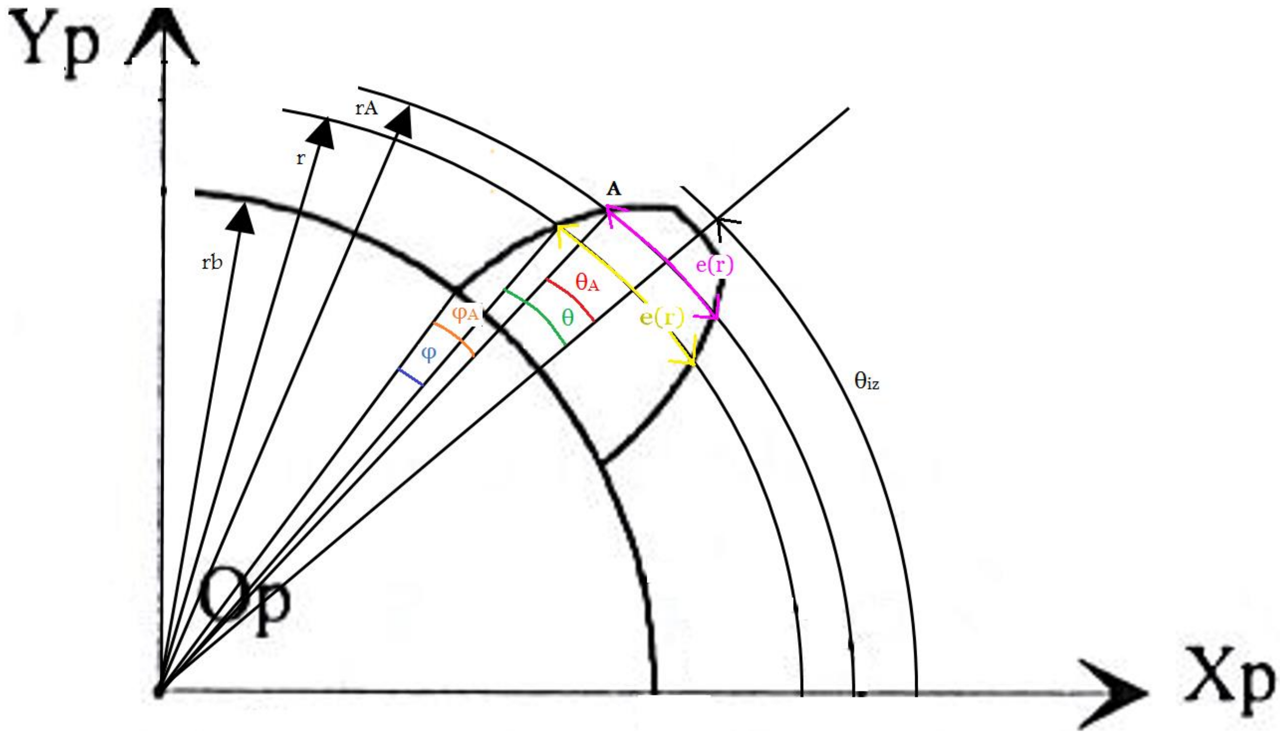

Fig.5.3 Aapparent plane of tooth

The angular coordinate $\boldsymbol{\theta_{iA}}$ is defined as follows:

$$\theta_{iA} = \theta_A + \theta_{iZ} \qquad (5.1)$$

Where:

rb base radius

r pitch radius

ra circumference radius to which point **A** belongs

e(r) apparent thickness of the tooth at the pitch radius

e(ra) apparent thickness of the tooth at radius **ra**

Through this system of equations:

$$\begin{cases} \theta_A = \theta + \varphi - \varphi_A \\ \theta = \dfrac{e(r)}{2r} \\ \varphi = inv(\alpha_t) \\ \varphi_A = inv(\alpha_{tA}) \\ e(r) = \dfrac{\pi m_t}{2} + 2x_1 m_n tan(\alpha_t) \end{cases}$$

It is possible to express θ_{iA} as follows:

$$\theta_{iA} = (i-1)\cdot\frac{2\pi}{Z} + \frac{tan(\beta_b)}{r_b}\cdot z_A + \rho\cdot(\frac{1}{2r}(\frac{\pi m_t}{2} + 2x_1 m_n tan(\alpha_t)) + inv(\alpha_t) - inv(\alpha_{tA})) \quad (5.2)$$

Where:

$$\alpha_{tA} = acos\left(\frac{r_b}{r_A}\right) \qquad (5.3)$$

Represents the apparent pressure angle of point **A** and depending on the side we are considering ρ we can have the following values:

$$\rho = \begin{cases} +1 \ \ left\ side \\ -1 \ \ right\ side \end{cases}$$

Defined the reference system of the helical pinion, it is possible to modeling the cutting kinematics.

5.2.2 Modeling of the hobbing kinematics

During the hobbing process, the hob and pinion rotate around their respective axes. The axes of rotation of the pinion and of the drill are not parallel, this allows to obtain a helical pinion. During the process, the pinion only performs a rotary movement around its own axis at a known angular velocity **Ωp**, the cutter rotates about its axis at a known angular velocity **Ωh** and at the same time translates to complete the pinion cutting.

The translation performed by the cutter takes place at a known speed **Vh**. We have not spoken directly of axial translation because the translation can take place in two different directions. We talk about the axial translation if the cutter moves along the axis of the cut pinion, we talk about the oblique translation if the hob moves along the direction of the toothing generated during the hobbing process according to an angle of inclination **β** between the axis of rotation of the pinion and the direction of advancement of the hob. Fig.5.4 shows the possible feed directions of the hob.

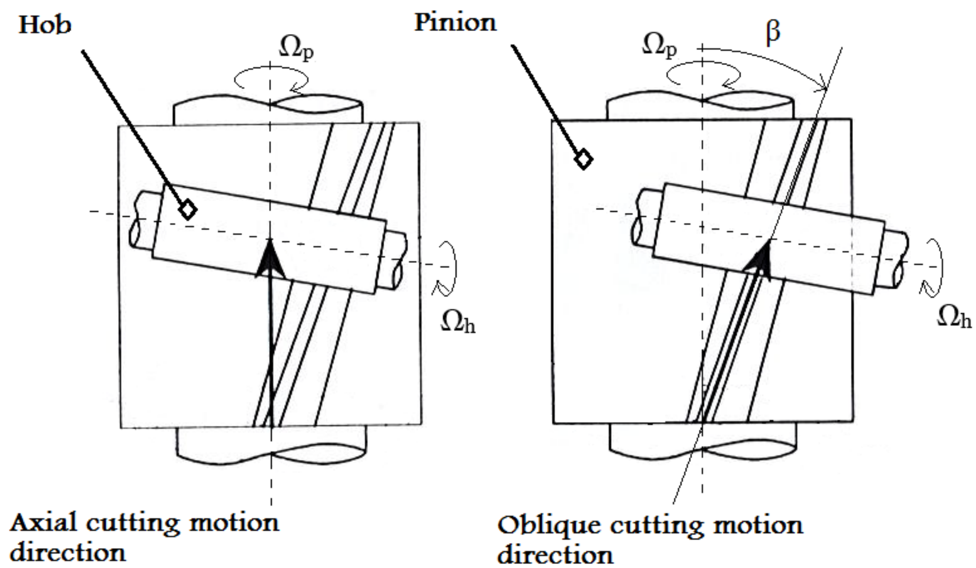

Fig.5.4 Hob feed directions[14]

To carry on the modeling of hobbing and grinding process, we need to establish the mathematical relationships between the pinion and the hob kinematics. We have defined a fixed local reference system for the pinion Rp0 defined by $\mathbf{n}_{xp0}$, $\mathbf{n}_{yp0}$, $\mathbf{n}_{zp0}$ and the origin $\mathbf{O_p}$. The fixed local reference system of the hob Rh0 is defined by $\mathbf{n}_{xh0}$, $\mathbf{n}_{yh0}$, $\mathbf{n}_{zh0}$ and the origin $\mathbf{O_h}$. Fig.5.5 shows the mutual position of the reference systems $\mathbf{R_{p0}}$ and $\mathbf{R_{h0}}$.

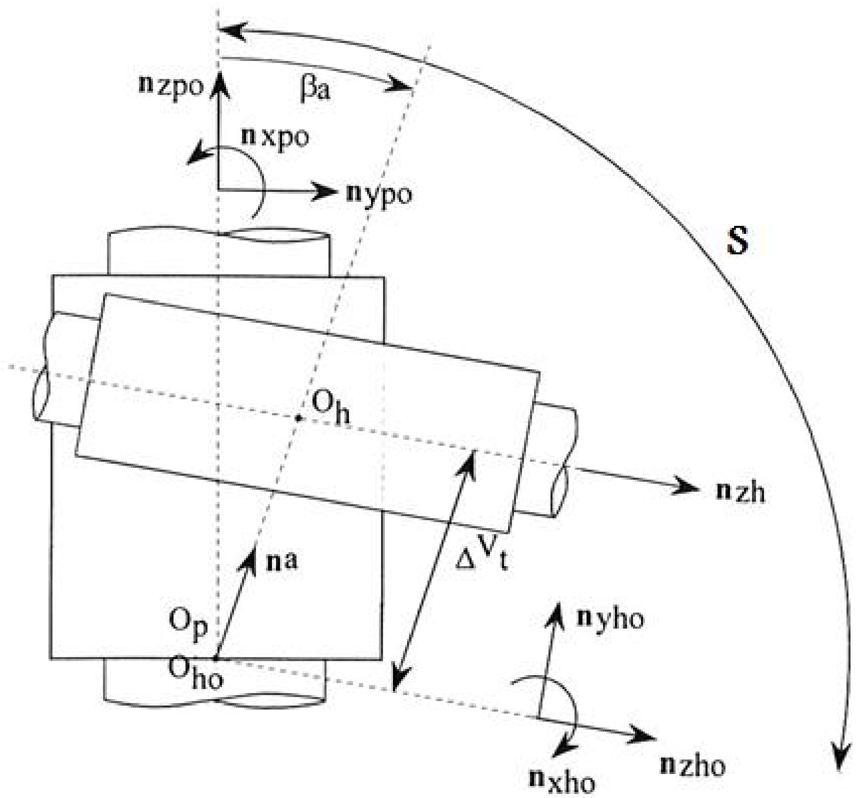

Fig.5.5 Mutual position of pinion and hob[14]

The cutting motion direction is done by the unit vector $\mathbf{n}_a$ and it is defined as follows:

$$\boldsymbol{n}_a = cos(\beta_a)\boldsymbol{n}_{z0} + sin(\beta_a)\boldsymbol{n}_{y0}$$

Depending on the type of feed **βa** will have the following values:

$\beta_a = \beta$ oblique cutting motion direction

$\beta_a = 0$ axial cutting motion direction

In modeling we assume that the feed is axial. The S coefficient represents the algebraic sum of the primitive helical angle of pinion and hob.

By defining with **θp** and **θh** the angular position of the pinion and the hob, respectively, during the hobbing process, it is possible to define a mobile local reference system for the pinion and for the hob. The fixed local reference system of the pinion **Rp0** is expressed as a function of the fixed local reference system **Rh0** as follows:

$$\boldsymbol{n}_{xp0} = -\boldsymbol{n}_{xh0}$$
$$\boldsymbol{n}_{yp0} = -cos(S)\boldsymbol{n}_{yh0} + sin(S)\boldsymbol{n}_{zh0}$$
$$\boldsymbol{n}_{zp0} = sin(S)\boldsymbol{n}_{yh0} + cos(S)\boldsymbol{n}_{zh0}$$

The local mobile reference system of the pinion Rp is expressed as a function of the fixed local reference system **Rp0** as follows:

$$\boldsymbol{n}_{xp} = cos(\theta_p)\boldsymbol{n}_{xp0} - sin(\theta_p)\boldsymbol{n}_{yp0}$$
$$\boldsymbol{n}_{yp} = sin(\theta_p)\boldsymbol{n}_{xp0} + cos(\theta_p)\boldsymbol{n}_{yp0}$$
$$\boldsymbol{n}_{zp} = \boldsymbol{n}_{zp0}$$

The local mobile reference system of the hob **Rh,** is expressed as a function of the fixed local reference system **Rh0**, as follows:

$$\boldsymbol{n}_{xh} = cos(\theta_h)\boldsymbol{n}_{xh0} + sin(\theta_h)\boldsymbol{n}_{yh0}$$
$$\boldsymbol{n}_{yh} = -sin(\theta_h)\boldsymbol{n}_{xh0} + cos(\theta_h)\boldsymbol{n}_{yh0}$$
$$\boldsymbol{n}_{zh} = \boldsymbol{n}_{zh0}$$

The angular positions **θp** and **θh** are not independent from each other so it is possible to express θh as a function of θp as follows:

$$\theta_h = -\frac{\pi}{z_2} - \frac{r_1}{r_2} \cdot \frac{cos(\beta_1)}{cos(\beta_2)} \cdot \theta_p \qquad (5.4)$$

Where **r1** and **r2** are the pitch radius of the pinion and the hob respectively.

5.2.3 Technical data for pinion and cutter

The pinion is generally defined by the following data:

- Number of teeth z_1
- Real Module m_n
- Real pressure angle α_n
- Primitive helix angle β_1
- Correction coefficient x_1

The hob is generally defined by the following data:

- Number of flutes z_2
- Number of gorge Nbg
- Real Module m_n
- Real pressure angle α_n
- Primitive helix angle β_2
- Correction coefficient x_2

The technical data provided by PSA show different values of real module and real pressure angle between pinion and hob. The real module and the real pressure angle between the pinion and the hob must be the same to allow the engagement.

The pinion data are related to a local reference system, therefore a translation of the technical data of the pinion in the reference system of the hob has been carried out. The hob manages the hobbing process and therefore the teeth created, for this reason the following considerations have been assumed:

a) Real pinion module equal to the real module of the hob
b) Real pinion pressure angle equal to the real pressure angle of the hob

Furthermore, the tip radius and root radius of the pinion, declared by PSA, have been maintained the same, because they belong to a real geometry and they do not depend on any reference system. Also, the base radius of the pinion, declared on the data sheet, has been maintained the same to keep the same involute of the helical tooth.

The $\mathbf{C_{fu}}$ coefficient has been assumed unitary. Starting from the module and the real pressure angle, the pinion data have been recalculated. The data taken by PSA data-sheet are represented without apex, the data recalculated are represented with apex.

The mathematical relationships for data transformation are the following[29]:

$\alpha_n' = \alpha_{nh}$	$\frac{tan(\beta_b)}{r_b} = \frac{tan(\beta_{b'})}{r_{b'}}$
$r_b' = r_b$	$sin(\beta') = \frac{sin(\beta_b{}')}{cos(\alpha_n{}')}$
$m_n' = m_{nh}$	$tan(\alpha_t{}') = \frac{tan(\alpha_n{}')}{cos(\beta')}$
$r_a' = r_a$	$m_t' = \frac{m_n{}'}{cos(\beta')}$
$r_f' = r_f$	$r_1' = \frac{m_t{}' z_1}{2}$
$C_a' = \frac{r_a{}' - r_1{}'}{m_n{}'} - x_1'$	$C_f' = \frac{r_1{}' - r_f{}'}{m_n{}'} + x_1'$
$s_t' = \frac{\pi\, m_t{}'}{2} + 2x_1'\, m_n' tan(\alpha_t')$	

The coefficient **x_1'** forms part of the pinion thickness formula and, to calculate the new value, several steps have been carried out as shown below:

a) Express the apparent base thickness, declared on PSA data sheet, in according to the pitch radius

$$s_{tb}=s_t(r_b) \rightarrow s_t(r_1)$$

$$s_t = \left(\frac{s_{tb}}{r_b} - 2inv(\alpha_t)\right) \cdot r_1 \qquad (5.5)$$

b) Equal the thickness calculated with the general thickness formula as a function of the recalculated pitch radius

$$s_t(r_1') \rightarrow s_t'$$

$$\frac{\pi\, m_t{}'}{2} + 2x_1'\, m_n' tan(\alpha_t') = \left(\frac{s_t}{2\, r_1} + inv(\alpha_t) - inv(\alpha_t')\right) \cdot 2r_1' \qquad (5.6)$$

c) Obtain x_1'

Through the PSA technical drawing of the hob, it has been possible to take the geometric data of the hob. The profile shift coefficient has been calculated starting from the thickness of the hob, and we obtained a null profile shift profile or the hob. Now we can begin to model the engagement between pinion and hob.

The modelling consists in the following steps:

I. Draw the pinion profile

II. Draw the hob profile

III. Draw the engagement between pinion and hob, obtaining tangent profiles

IV. Get contact points on the wheel surface during the grinding process

V. Get contact points on the hob surface during the grinding process

VI. Get contact points on the wheel surface during the hobbing process

VII. Get contact points on the hob surface during the hobbing process

6
Results

In this section, the results about the modelling of hobbing and grinding process will be shown and explained.

6.1 Helical pinion drawing

The equation (5.2) allows to trace the profile of the tooth on the apparent plane. The vector **rm1** defines the value of the radius cylinder on which calculate the tooth profile. We introduced a factor **dec** to represent the desplacement to be carried out to report the tooth profile on the origin of the reference system **Rp0**. A null dec means tracing the tooth profile on a reference system that is shifteed by half the thickness of the tooth. To return the tooth drawn on the origin of reference system **Rp0**, a translation equal to dec is necessary.

After defining the profile of a pinion tooth on the **Xp0** and **Yp0** plane with **Zp0** null, the matrices **MX1, MY1, MZ1** have been created to define the **3D** profile of the pinion tooth. The vector **tz** defines the extension of the tooth on the **Zp0** axis, then its width. Fig.6.1 shows the tooth profile of the helical pinion.

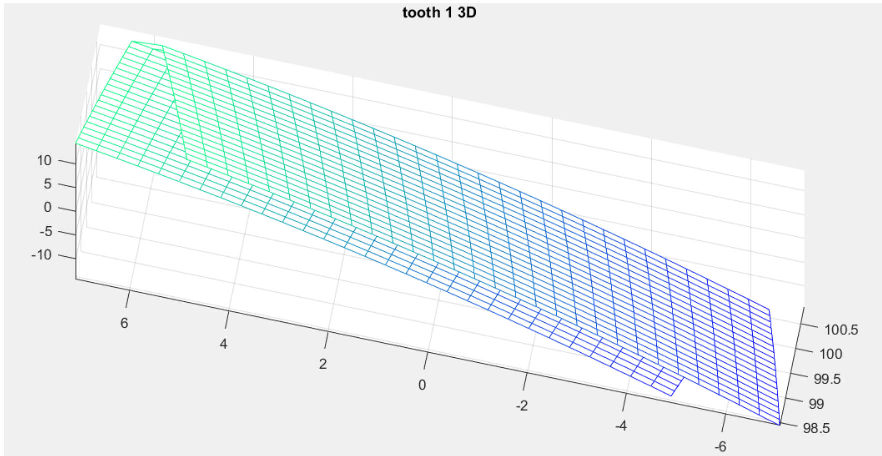

Fig.6.1 Tooth profile of helical pinion

After defining the three-dimensional structure of the pinion tooth, the **M2X1, M2Y1, M2Z1** matrices have been defined to generate the three-dimensional structure of the pinion. The following teeth are designed in according to a circular pitch **p**. Fig.6.2 shows the pinion.

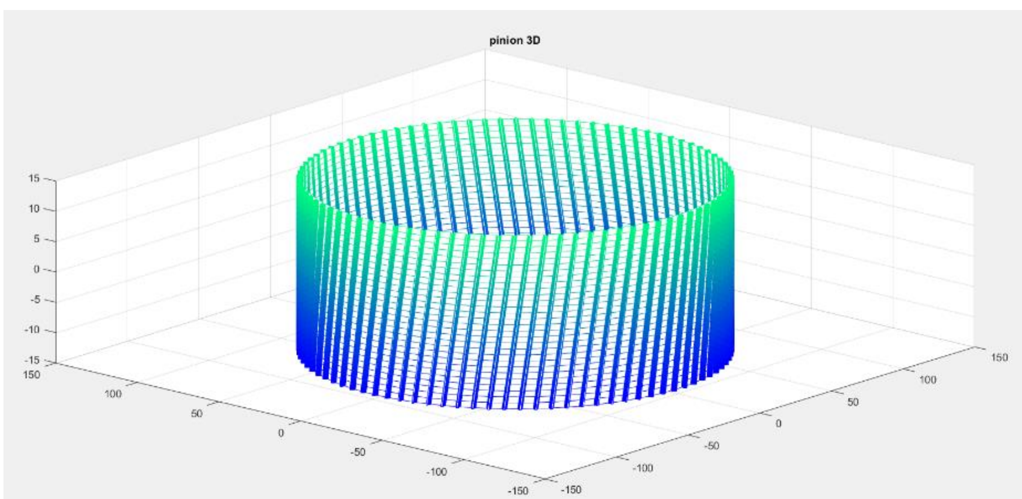

Fig.6.2 Helical pinion

6.2 Hob drawing

For the hob geometrical modelling, it is possible to consider the hob as a wheel. Then, it is possible to consider the engagement between the hob and the pinion as an engagement between two helical wheels. For these reasons, the process of modelling the hob profile is the same used for the pinion previously. The **rm2** vector defines the value of the radius cylinder on which calculate the tooth profile of the hob.

After defining the fillet profile of the hob on the **Xh0** and **Yh0** plane with **Zh0** null, the matrices **MX2, MY2, MZ2** have been created to define the 3D profile of the hob fillet. The vector **tz2** has been defined to define the extension of the fillet on the axis **Zh0**, then its width. Fig.6.3 shows the hob fillet.

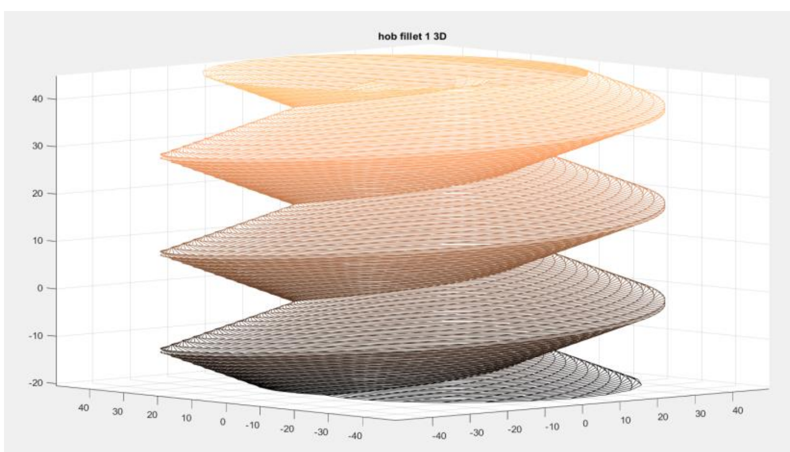

Fig.6.3 Hob fillet

After defining the three-dimensional structure of the hob fillet, the **M2X2, M2Y2, M2Z2** matrices have been defined to generate the three-dimensional structure of the hob. The following fillets are designed in according to a circular pitch **p**. Fig.6.4 shows the hob.

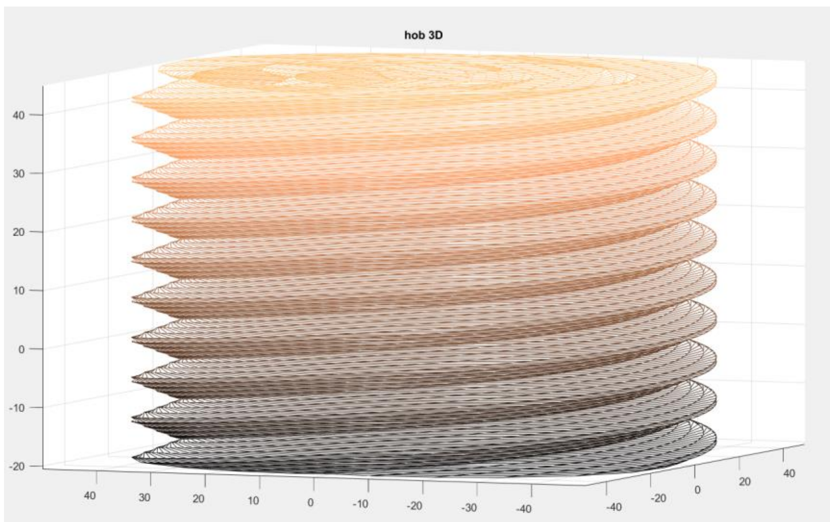

Fig.6.4 Hob

6.3 Pinion-Hob engagement

The interaxial distance between pinion and hob is not given by the sum of their pitch radius, but we must consider a distance given by the shift profile coefficient of pinion and hob. This interaxial distance **DC** is shown in Fig.6.5.

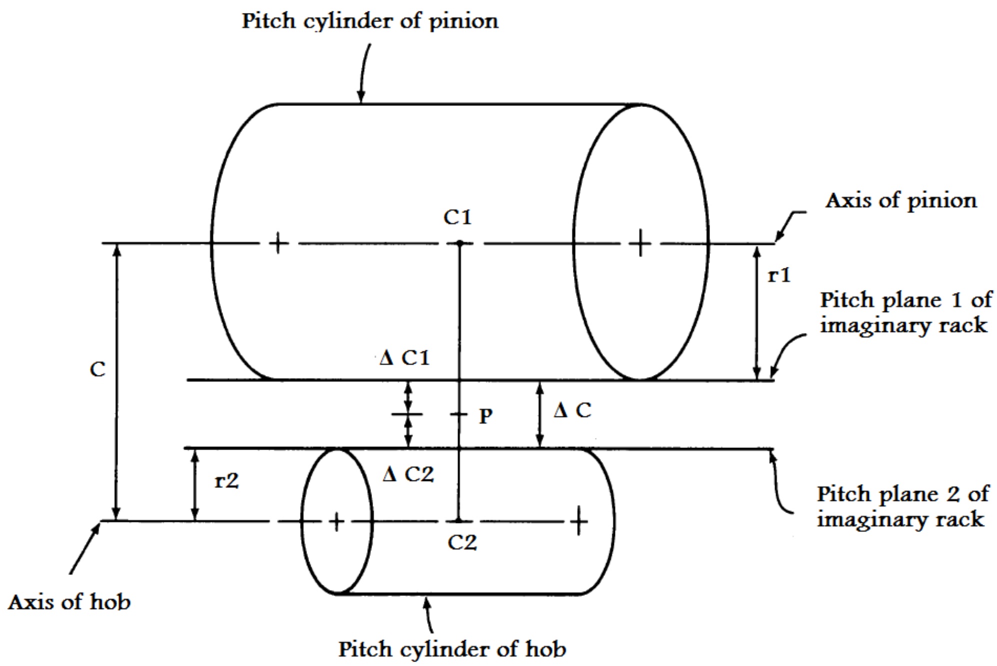

Fig.6.5 Interaxial distances[13]

After defining the interaxial distances, the initial angular positions of the pinion and the hob have been defined.

The initial angular position of the pinion is null and the initial angular is as follows:

$$\theta_{h0} = \frac{-\rho\pi}{z_2} \qquad (6.1)$$

During the hobbing and grinding process, the mobile reference system of each component rotates around its rotation axis **Z** according to an angle **θ**.

After expressing **Rp** and **Rh** in function of **Rp0** and **Rh0** respectively, the goniometric relations have been defined to express **Rh0** as a function of **Rp0**.

A generic point **M** is defined in **Rh0** as follows:

$$\overline{O_h M_h} = x_h \boldsymbol{n}_{xh0} + y_h \boldsymbol{n}_{yh0} + z_h \boldsymbol{n}_{zh0} \qquad (6.2)$$

The same point **M** with respect to **Rp0** is defined as follows:

$$\overline{O_p M_h} = \overline{O_p O_h} + \overline{O_h M_h} \qquad (6.3)$$

Where:

$\overline{O_p O_h} = C\ \boldsymbol{n}_{xp0}$

$\boldsymbol{n}_{xh0} = -\boldsymbol{n}_{xp0}$

$\boldsymbol{n}_{yh0} = -cos(S)\boldsymbol{n}_{yp0} + sin(S)\boldsymbol{n}_{zp0}$

$\boldsymbol{n}_{zh0} = sin(S)\boldsymbol{n}_{yp0} + cos(S)\boldsymbol{n}_{zp0}$

Through the relationships listed above, it is possible to express **Rh0** in **Rpo**. Fig.6.6 shows the engagement between pinion and hob.

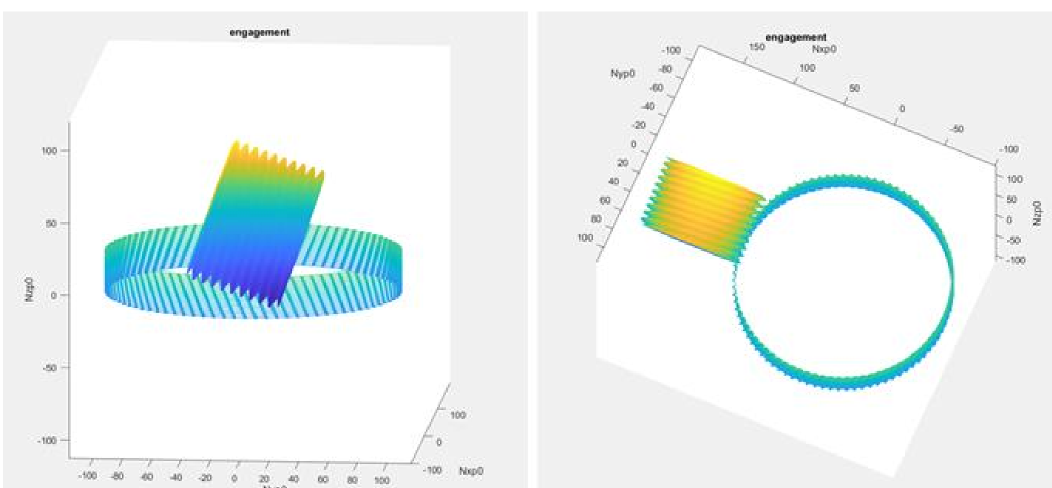

Fig.6.6 Pinion-Hob Engagement

6.4 Contact points during grinding process

The code to modelling the hobbing and grinding process could be considered the same. This is possible because both processes work following similar dynamics.

The main difference between the hobbing and grinding process are:

- Hobbing process: non-continuous process
- Grinding process: continuous process

The procedure to obtain the contact points between pinion and hob depends on the manufacturing process.
The kinematic data of the machine have been defined as follows:
Ω_p=1 rpm
fh=0.2 mm/turn

The matrices have been defined to save the contact points.
The feed speed of the hob **Vh** is related to the angular speed of the pinion, and is defined as follows:

$$V_h = \frac{\Omega_p}{2\pi} f_h \qquad (6.4)$$

Between **Ωp** and **Ωh** there is a relationship depending on the type of cutting motion direction. The relation is[14]:

$$\Omega_h = -\frac{z_1}{z_2}\left[\Omega_p + \frac{tan(\beta_{1b})}{r_{1b}}\left(\frac{sin(S-\beta_a)}{sin(S)} - \frac{sin(\beta_2)sin(\beta_a)}{sin(\beta_1)sin(S)}\right)\cdot V_h\right] \qquad (6.5)$$

In our case, the feed is axial.

The manufacturing process is not instantaneous but last for a certain time, for this reason a vector of time tt has been defined. To define the vector **tt** it is necessary to start from the definition of angular position of the pinion at the time **θpt**[14]:

$$\theta_{pt} = \theta_p + \frac{tan(\beta_{1b})}{r_{1b}} z_{pt} + (i-1)\frac{2\pi}{z_1} \qquad (6.6)$$

With:

$$\theta_p = \Omega_p \cdot t \qquad (6.7)$$

$$z_{pt} = \frac{sin(S-\beta_a)}{sin(S)}\Delta V_t \qquad (6.8)$$

$$\Delta V_t = V_h \cdot t \qquad (6.9)$$

ΔVt represents the movement of the cutter along the feed direction, in the case of axial feed, **ΔVt** will be equal to **zpt**. The rotation of the pinion is reversed with respect to the convention initially applied, so the index the factor **(i-1)** will have a negative sign.

The index **i** does not represent the tooth-i th but represents the transition from one tooth to the next during the process, therefore the **ii-th** index does not correspond to the real tooth ii-th but the relation between **i** and **ii** is:

ii=1 → i=1

ii=2 → i=z_1

ii=3 → i=z_1-1

It is possible to rewrite **θpt** as follows:

$$\theta_{pt} = \Omega_p \cdot t + \frac{tan(\beta_{1b})}{r_{1b}} \frac{\Omega_p f_h}{2\pi} \cdot t - (ii - 1) \frac{2\pi}{z_1} \qquad (6.10)$$

It is possible to obtain $t: \theta_{pt}(ii, z_{pt}, t) = 0$ as follows:

$$t = \frac{(ii-1)}{\Omega_p} \frac{2\pi}{z_1} \left(\frac{1}{1 + \boxed{\frac{tan(\beta_{1b})}{r_{1b}} \frac{f_h}{2\pi}}} \right) \qquad (6.11)$$

The term highlighted is a term **<< 1,** so we can use the first-degree development of Taylor and then get:

$$t = \frac{(ii-1)}{\Omega_p z_1} \cdot \left(2\pi - \frac{tan(\beta_{1b})}{r_{1b}} f_h \right) \qquad (6.12)$$

In similar way, the angular position of the hob over time is defined as follows:

$$\theta_{ht} = \theta_h + \frac{tan(\beta_{2b})}{r_{2b}} z_{ht} + (i_h - 1)\frac{2\pi}{z_2} \qquad (6.13)$$

With:

$\theta_h = \Omega_h \cdot \ t + \theta_{h0} \qquad (6.14)$

$z_{ht} = -\frac{sin(\beta_a)}{sin(S)} \Delta V_t \qquad (6.15)$

$\Delta V_t = V_h \cdot \ t \qquad (6.16)$

Subsequently, a verification is performed taking into consideration the relation reported[13]:

$$r_1 cos(\beta_1) \cdot \theta_{pt} + r_2 cos(\beta_2) \cdot \theta_{ht} + \frac{1}{2}(e_{n1} + e_{n2}) = \Delta C \cdot tan(\alpha_n) \qquad (6.17)$$

Once the angular positions of pinion and hob have been defined, the coordinates of the contact points on the surface of pinion and hob have been determined.

The following discussion refers to the pinion, but similarly has been done for the hob, as reported in the code. We represent with **zm** the coordinate of the point of contact on the surface of the pinion, and it is defined as follows:

$$z_m = z_{mt} + z_{pt} \qquad (6.18)$$

Zpt has been defined previously, such as the hobbing or grinding coordinate on the pinion profile at time t. **Zmt** represents the coordinate of the point of contact **M** starting from point **C1** belonging to the axis of rotation of the pinion, and it is defined as follows[13]:

$$z_{mt} = \frac{1}{tan(\beta_{b1})}\left(s_1 - r_{b1} \cdot \left(\theta_{pt} + w_1 \frac{\pi}{2z_1}\right)\right) \qquad (6.19)$$

The term **w1** represents a scaling factor of the theoretical tooth thickness. In the case of the hob, the thickness scale factor is unitary. To define **zmt** it is therefore necessary to define s1. **S1** is the distance between the point of contact **M** and the point **P** belonging to the line of action as shown in Fig.6.7.
S1 is defined as follows[13]:

$$\frac{s_1}{cos(\beta_{b1})} = cos(\alpha_n)\left(\frac{\Delta C_1}{tan(\alpha_n)} + \frac{1}{2}e_{n1} + r_1 cos(\beta_1)\theta_{pt}\right) \qquad (6.20)$$

In similar way, **s2** is defined for the hob.

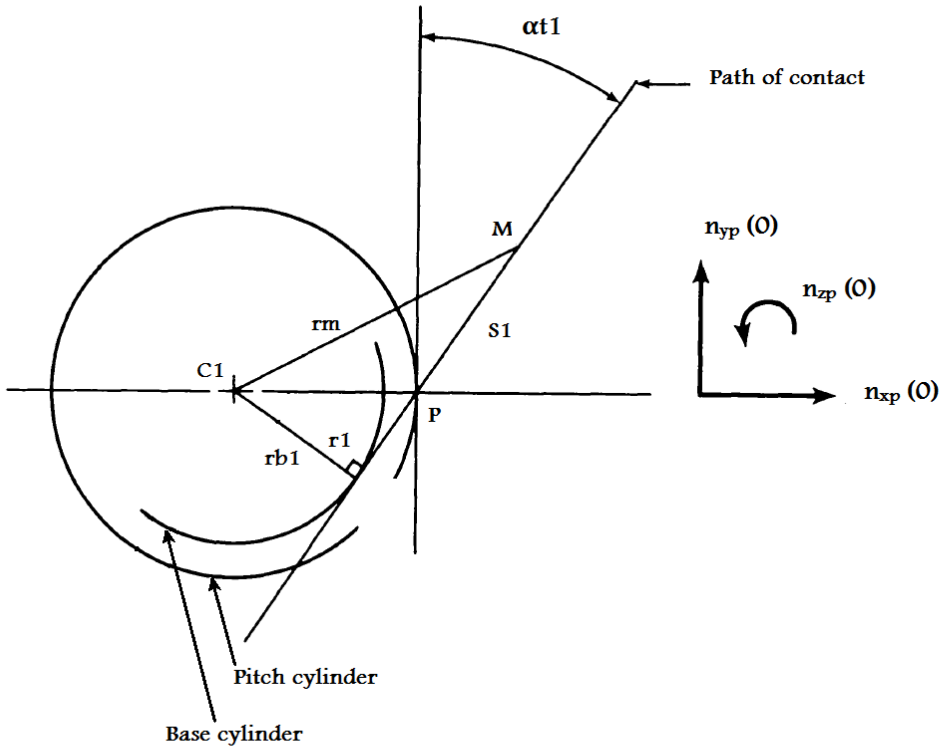

Fig.6.7 Point of contact[13]

S1 can be expressed as a function of the apparent pressure angles of the contact point and pitch radius, as follows[14]:

$$s_1 = r_{b1}\big(tan(\alpha_{tm1}) - tan(\alpha_{t1})\big) \qquad (6.21)$$

Subsequently, a further check has been performed to ensure consistency between the differents mathematical relationships.

To have a correct engagement and correct contact points it is necessary to verify this relation[14]:

$$\frac{r_{b1}}{cos(\beta_{b1})}\left(tan(\alpha_{tm1})-tan(\alpha_{t1})\right)+\frac{r_{b2}}{cos(\beta_{b2})}\left(tan(\alpha_{tm2})-tan(\alpha_{t2})\right)=\frac{\Delta C}{sin(\alpha_n)} \quad (6.22)$$

To obtain the **xm** and **ym** coordinates of the contact point **M**, a vector rm has been defined. It represents the radius with center in **C1** on which the different contact points are positioned, as shown in Fig.6.7. On the apparent plane of the tooth, a point of contact is also a point of cutting or grinding.

In the code **θm** it has a negative sign, because the sense of rotation of the pinion is reverse. A verify has been done to ensure **rm** between the tip radius and root radius. In a similar way, the coordinates of the contact points belonging to the hob have been obtained.

The matrices that have been obtained [Mpx, Mpy, Mpz] and [Moux, Mouy, Mouz] are respectively the matrices of the contact points during the grinding process belonging to the surface of the pinion and the hob.
Fig.6.8 shows the contact points on each tooth of the pinion and on the hob.

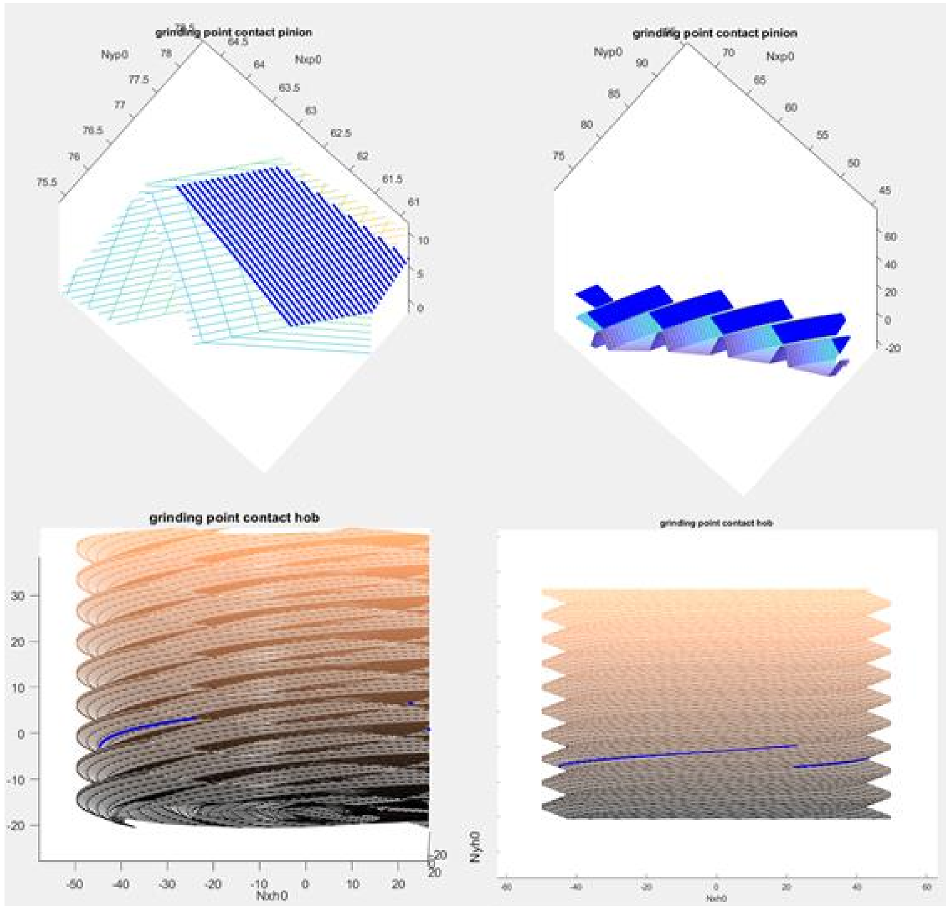

Fig.6.8 Grinding contact points

6.5 Contact points during the hobbing process

To obtain contact points during the hobbing process we must select the contact points that we have previously obtained. The selection criterion is based on the flutes: a point of contact is also a cutting point if this point belongs to a flute of the hob. As mentioned previously, the hobbing process is not a continuous process but there are stops when moving from one flute to the next, so the cutting points are exclusively the points belonging to the flute.

To select the points of cutting, it depends on the type of flute Fig.6.9:

- Helical flute
- Straight flute

The flute developed along the perpendicular of the hob fillet are called helical flute. The flute developed along the axis of rotation of the hob are called straight flute.

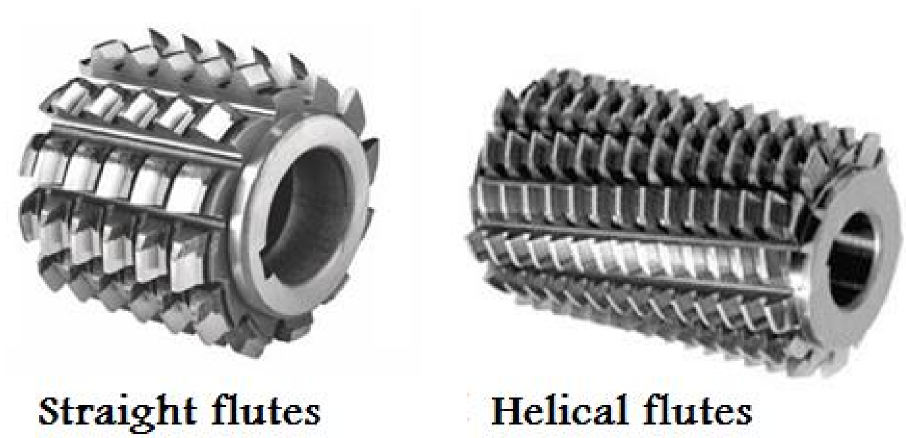

Fig.6.9 Straight and helical flutes[30]

A straight flute does not allow to obtain an optimal hobbing process as it could be with a helical flute hob, but the process of sharpening on straight flute hob is certainly less complicated than a helical flute hob.

We have a hob with straight flutes, then we consider the relation as follows:

A point **M**, belonging to the hob whose cylindrical coordinates are $\{\mathbf{r_{mh}}, \boldsymbol{\theta_{mh}}, \mathbf{z_{mh}}\}$, is a cutting point if its cylindrical coordinates satisfy the equation of belonging to flute k-th [14]:

$$\theta_{mh} = \theta_{k0} + (k-1) \cdot \frac{2\pi}{N_{bg}} \qquad (6.22)$$

The matrices that have been obtained [M_{p2x}, M_{p2y}, M_{p2z}] and [M_{ou2x}, M_{ou2y}, M_{ou2z}] are respectively the matrices of the contact points during the hobbing process belonging to the surface of the pinion and the hob. Fig.6.10 shows the contact points on each profile of pinion and hob.

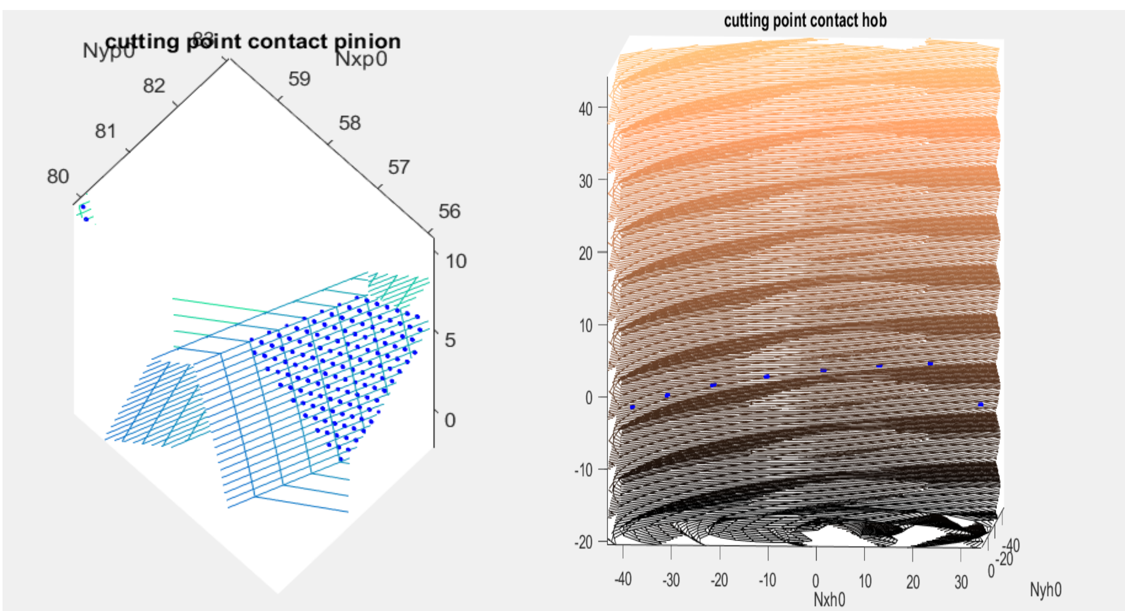

Fig.6.10 Hobbing contact points

7

Conclusion

7.1 Project development

The project was based on an accurate theoretical study on the phenomenon of sound in speed reducers, which is a current study and takes in many companies in the automotive sector. The main causes that have been attributed to the sound phenomenon are manufacturing defects that inevitably lead to geometric defects of components that are part of a gear. For this reason, it was decided to analyze the hobbing process and the grinding process to which a tooth wheel is usually subjected.

In order to analyze the hobbing and grinding process, a detailed study was carried out on the hobbing kinematics of a pinion through a hob. The data characterizing the pinion and the hob are real. In order to model the hobbing process that generates the helical wheel, the kinematic relations between the hob and the pinion have been studied during the engagement.

A matlab code was implemented to generate the pinion and the hob in three dimensions, then the engagement conditions were defined, and the theoretical contact points were then obtained during the hobbing and grinding process on the surface of the pinion and on the surface of the hob. To draw the gear models by MATLAB codes is difficult at the beginning. Firstly, all the functions and relationships of gear curves should be found out from mathematic and geometric point of view. Secondly, all the curves of gear models are made up of a series of nodes in matrix form, so how to handle with matrix operation like matrix addition, matrix rotation should be learnt. Thirdly, proper MATLAB programming languages and functions should be used, such as ‘for’ loop codes, ‘flip’ function, ‘cat’ function, and ‘mesh’ function etc.

7.2 Forthcoming objectives

Now that the modelling code of the hobbing and grinding process has been written, it will be possible to subsequently extrapolate the theoretical contact points and compare these with the real contact points and note any differences. To understand the possible difference between the theoretical and the actual simulation, it will be necessary to introduce some tooth profile modification on the gear models, based on the theoretical study carried out in the project on the different types of defects. This is possible because MATLAB can import data from .mat file.

Then, every time doing the tooth profile modification, just load the tooth profile modification code files to the tooth model files, the model with tooth profile modification can be obtained. By MATLAB GUI it is possible to provide a more straight and simpler way for users to obtain gear models and to do tooth profile modification, because users just must input and click buttons in the interface without knowing the programming codes.

Subsequently it will be necessary to obtain the meshing frequencies between the theoretical engagement and the real engagement and to understand which of the different defects introduced gives a theoretical result close to the real one.

Bibliography

1. Henriksson M. On noise generation and dynamic transmission error of gears. 2009.

2. Uicker JJ, Pennock GR, Shigley JE, Shigley JE. *Theory of Machines and Mechanisms*. 3rd ed. New York: Oxford University Press; 2003.

3. Systematic Approach to Finding the Best Transmission Variant – IAV Automotive Engineering. https://www.iav.com/en/automotion-magazine/automotion-2016-03/systematic-approach-finding-best-transmission-variant. Accessed January 21, 2019.

4. Singh R. A brief review of transmission in automobiles. *Int J Latest Res Sci Technol ISSN*. 1:222-226. http://www.mnkjournals.com/ijlrst.htm. Accessed January 21, 2019.

5. A & M Gearbox Services Limited in Chelmsford. https://19da400b_aandm_.multiscreensite.com/. Accessed January 21, 2019.

6. Torque converter, CVT, dual or single clutch autos, what's the difference? - Car Advice | CarsGuide. https://www.carsguide.com.au/car-advice/torque-converter-cvt-dual-or-single-clutch-autos-whats-the-difference-33411. Accessed January 21, 2019.

7. Vehicle Transmission Types and Their Differences | AxleAddict. https://axleaddict.com/auto-repair/Vehicle-Transmission-Types-and-Their-Differences. Accessed January 21, 2019.

8. Automatic Transmission | Cars.com. https://www.cars.com/auto-repair/glossary/automatic-transmission/. Accessed January 21, 2019.

9. Official website. *Peugeot Citroën Moteurs*. http://www.peugeot-citroen-moteurs.fr/en-gb/. Accessed January 23, 2019.

10. Yuan LIU, Zhen GUO, Yao Z. Error Analysis on CNC gear hobbing Machine Spindle Transmission Chain Based on SOV Theory. 2015;(Aemt):209-217.

11. Woodbury RS. *History of the Gear-Cutting Machine: A Historical Study in*

Geometry and Machines. MIT Press; 1958. https://books.google.com/books?id=YxEVAAAAMAAJ. Accessed January 21, 2019.

12. Satayotin K. Gear Tooth Profile Error caused by Hob Misalignment. 2013;6:51-55.

13. J.R. Colbourne. *The Geometry of Involute Gears*. (Springer-Verlag, ed.).; 1987.

14. Eric Chermet. Contribution à l'analyse et à la modelisation des ecarts geometriques sur les dentures d'engranages cylindriques tailles par fraise-mere. 1997.

15. Banodiya B, Kumar Karma V. MEASURMENT OF TRANSMISSION ERROR IN SPUR GEARS. *Int Res J Eng Technol*. 2017. www.irjet.net. Accessed January 21, 2019.

16. Errore di trasmissione - Wikipedia. https://it.wikipedia.org/wiki/Errore_di_trasmissione. Accessed January 21, 2019.

17. R.K.Gupta. *Manufacturing Engineering*.

18. Gleason Corporation. Threaded Wheel Grinding Machines The Platform for Automotive Gearbox Parts and More. :1-8.

19. Hob Rake Error - As the Gear Turns. https://asthegearturns.com/2013/12/11/hob-rake-error/. Accessed January 21, 2019.

20. Hine K, Nilsson AI. *Improving Landfill Monitoring Programs with the Aid of Geoelectrical-Imaging Techniques and Geographical Information Systems Gear Whine Noise Excitation Model*. http://publications.lib.chalmers.se/records/fulltext/175061/175061.pdf. Accessed January 21, 2019.

21. Centers PM. KLINGELNBERG.

22. Akerblom M. Gearbox Noise − Correlation with Transmission Error and Influence of Bearing Preload. 2008.

23. Kostić SĆ. The Noise Structure of Gear Transmission Units and the Role of Gearbox Walls. 2007:105-112.

24. ISO 1328-1:2013(en), Cylindrical gears — ISO system of flank tolerance classification — Part 1: Definitions and allowable values of deviations relevant

to flanks of gear teeth. https://www.iso.org/obp/ui/#iso:std:iso:1328:-1:ed-2:v1:en. Accessed January 21, 2019.

25. Henriot G. Influence des ondulations de surface des dentures sur le bruit. 2000;2139:477-486.

26. *Mathworks.Com Company Overview*.; 2018. https://www.mathworks.com/content/dam/mathworks/tag-team/Objects/c/company-fact-sheet-8282v18.pdf. Accessed January 21, 2019.

27. What is CATIA? | Professional industrial design services, High value-added mold and High quality product suppliers. https://www.firstratemold.com/what-is-catia/. Accessed January 21, 2019.

28. Fuentes A, Ruiz-Orzaez R, Gonzalez-Perez I. Computerized design, simulation of meshing, and finite element analysis of two types of geometry of curvilinear cylindrical gears. *Comput Methods Appl Mech Eng*. 2014;272:321-339. doi:10.1016/j.cma.2013.12.017

29. Dufailly J, Boucard P-A. *Engrenages Cylindriques de Transmission de Puissance : Étude Géométrique*. Ellipses; 2016.

30. Gear Hob Cutter at Rs 3500 /piece | Focal Point | Patiala | ID: 6940546762. https://www.indiamart.com/proddetail/gear-hob-cutter-6940546762.html. Accessed January 22, 2019.